Energy 305 (2024) 132366

Contents lists available at ScienceDirect

Energy

journal homepage: www.elsevier.com/locate/energy

Mathematical optimization modeling for scenario analysis of integrated steelworks transitioning towards hydrogen-based reduction

Carl Haikarainen [a,*], Lei Shao [b], Frank Pettersson [a], Henrik Saxén [a]

[a] Process and Systems Engineering Laboratory, Åbo Akademi University, Åbo, Finland
[b] School of Metallurgy, Northeastern University, Shenyang, 110819, China

ARTICLE INFO

Handling editor: Neven Duic

Keywords:
Steel production
Optimization
MINLP
Transition
Hydrogen
System model

ABSTRACT

To reduce carbon dioxide emissions from the steel industry, efforts are made to introduce a steelmaking route based on hydrogen reduction of iron ore instead of the commonly used coke-based reduction in a blast furnace. Changing fundamental pieces of steelworks affects the functions of most every system unit involved, and thus warrants the question of how such a transition could optimally take place over time, and no rigorous attempts have until now been made to tackle this problem mathematically. This article presents a steel plant optimization model, written as a mixed-integer non-linear programming problem, where aging blast furnaces and basic oxygen furnaces could potentially be replaced with shaft furnaces and electric arc furnaces, minimizing costs or emissions over a long-term time horizon to identify possible transition pathways. Example cases show how various parameters affect optimal investment pathways, stressing the necessity of appropriate planning tools for analyzing diverse cases.

1. Introduction

Steel production currently stands for about 7 % of anthropogenic CO_2 emissions [1], which has motivated efforts to find alternative and more sustainable ways of producing steel. One suggested remedy has been to replace coke-based reduction in blast furnaces followed by conversion of hot metal into steel in basic oxygen furnaces (the BF-BOF route) by hydrogen-based reduction in shaft furnaces followed by melting of the resulting direct reduced iron (DRI) in electric arc furnaces (the H2-SF route) [2]. Both these routes start from iron ore as raw material and result in crude steel that can be further processed into steel products. While the BF-BOF route relies on coal both as a reducing agent and as a source of energy, the H2-SF route requires hydrogen for the reduction and large amounts of electricity as an energy source, both in the electric arc furnaces and for producing the hydrogen, when done through electrolysis. Challenges in large-scale realization of the H2-SF route include the availability of low-carbon electricity and the demand of higher-grade iron ores compared to the BF-BOF route.

Ongoing projects are implementing hydrogen direct reduction. The HYBRIT demonstration project in Sweden aims at replacing blast furnaces with shaft furnaces producing DRI pellets using hydrogen from electrolyzers powered by fossil-free electricity [3], followed by electric arc furnaces (EAF). The HYFOR pilot plant in Austria uses hydrogen gas to reduce iron ore concentrate fines, for further processing in an EAF or into hot briquetted iron [4]. The H2Stahl project in Germany aims at large-scale delivery of hydrogen via pipelines to supply hydrogen both for use in blast furnaces and for direct reduction [5]. These types of pilot projects contribute to the development of hydrogen-based steel production, and generally to large-scale utilization of hydrogen.

The hydrogen reduction process has been studied from different points of view. Spreitzer and Schenk [6] reviewed the process and related literature and concluded that single process mechanisms are well known, but the combined process, with many influencing parameters, is not. Patisson and Mirgaux [7] presented a mathematical model for shaft furnace operation with hydrogen and experimental studies of iron ore reduction kinetics, and found that complete metallization could be achieved faster in reduction with only H_2 compared with reduction with both H_2 and CO. Using a kinetic model of a shaft furnace with top gas recycling, Shao et al. [8] found that productivity is higher in a shaft furnace with hydrogen than with syngas, further suggesting a dual-row injection of the reduction gas to improve thermochemical conditions and thus performance. Further experimental studies and experiences from pilot projects are expected to improve future shaft furnace models as well.

* Corresponding author.
E-mail address: carl.haikarainen@abo.fi (C. Haikarainen).

https://doi.org/10.1016/j.energy.2024.132366
Received 27 September 2023; Received in revised form 15 April 2024; Accepted 7 July 2024
Available online 8 July 2024
0360-5442/© 2024 The Authors. Published by Elsevier Ltd. This is an open access article under the CC BY license (http://creativecommons.org/licenses/by/4.0/).

Vogl et al. [9] analyzed a steelmaking process based on hydrogen direct reduction and compared its competitiveness against an integrated steel plant using the traditional BF-BOF route with different costs for electricity and CO_2 emissions and different charges of scrap in the EAF. They concluded that competitiveness of the hydrogen-based process highly depends on the availability of very low-cost electricity and/or high penalties for CO_2 emissions. They also studied break-even values for grid emission intensity (GEI) when the emissions for the H2-SF route equal emissions from the BF-BOF route, reaching the value 532 kgCO2/MWh with 100 % DRI charge to the EAF. Bhaskar et al. [10] made a techno-economic assessment of a hydrogen-based steel plant in Norway, with relatively cheap and fossil-free electricity largely available. Electricity prices in the study revolve around 30–50 €/MWh, and the authors found the H2-SF route about 40 % more costly than a corresponding BF-BOF route, with CO_2 mitigation costs of 68–180 US$/$t_{CO2}$ depending on plant configurations.

Effects of a transition towards hydrogen-based steel production considering energy system requirements have been studied by Pimm et al. [11]. They combined a model of steel production with a long-term energy system planning model to evaluate costs of hydrogen-based steel production, acknowledging the influence of scrap utilization rates in EAFs. Interaction between steel plants and the energy systems they are part of is important to consider, as intermittent renewable energy sources combined with production of hydrogen and steel can involve complex dynamics. System complexities are further increased if, e.g., valorization of byproducts and process gases is considered. Zaccara et al. [12] highlight the use of hydrogen in potential methanol and methane syntheses from steelworks off-gases, and Angeli et al. [13] studied a process for producing syngas from blast furnace and coke oven gases. Including this type of processes in a system analysis increases potential system flexibility and performance, but also makes the analysis much more complex.

The BF-BOF route in an integrated steel plant is well-established and optimized on a system level, utilizing process gases and by-streams efficiently. Changing the fundamental units in a steel plant will require rethinking the system with its various unit interactions to properly design and dimension new units as well as reconfigure old units preserved in the system. Optimized operation of integrated steel plants has been studied by, e.g., Ghanbari et al. [14], and similar modelling methodologies could be used for plants applying hydrogen-based reduction and plant configurations in intermediate stages of a transition. Transition pathway models have been studied in the context of energy systems by, e.g., Prina et al. [15], who developed a model for long-term energy planning, optimizing investments and operation of the Italian energy system over a selected time horizon, and by Haikarainen et al. [16], who developed an energy system transition model implemented as a mixed-integer linear programming problem. Both studies optimize long-term time horizons divided into shorter time steps. This type of transition pathway optimization has not yet been applied to steel production.

This article contributes to the literature by presenting an optimization modelling approach that can be used for analyzing investments and operation during a period in which a steel plant is considering transition to hydrogen-based reduction of iron ore to suppress emissions. As the approach is novel in this context, the model is presented in detail and its functionality is demonstrated with example cases. Section 2 of this article describes the optimization model with its objective function and constraints. The optimization minimizes accumulated costs or emissions over a time horizon, allowing for a comparison of different future scenarios for different types of plant configurations, with different assumptions regarding raw material availability and costs, electricity and carbon permit costs, grid emission intensities, etc. This type of a tool can provide information on potential combinations of investments and operational schemes involving old and new process units and streams, including raw materials and process by-products, that otherwise could be difficult to deduce in a complex transitional phase of an industrial site. Section 3 demonstrates model functionality with three example cases in which an integrated steel plant considers transitioning from blast furnaces to hydrogen-based reduction. Two cases compare a situation where an upcoming dismantling of blast furnaces has already been decided to one where prolonged blast furnace use is an alternative. A third case provides an additional comparison with higher costs placed on CO_2 emissions. The cases allow comparison of different steelmaking routes to identify key parameters affecting optimization outcomes. The article finishes with conclusions and future prospects in Section 4.

Nomenclature

Variables		Units
$\dot{m}$	Mass flow	t/h
$\dot{V}$	Volume flow	kNm^3/h
x	Fractions and rates	
T	Temperature	K, °C
P	Electrical power	MW
$\dot{Q}$	Heat flow	MW
H	Enthalpy flow	MW
S	System unit maximum capacity	
p	Pressure	kPa
d	Diameter	m
b	Binary selection variable	
y	Binary existence variable	
n	Integer decision variable	
C	Costs	€
Coefficients and parameters		
a	Annuity factor	
n	Amount	
c	Cost parameter	€, €/t, €/kNm^3, etc.
K	Equation coefficient	
h	Specific enthalpy	MJ/kg
η	Efficiency	
M	Big-M coefficient	
λ	Hydrogen input rate	
Subscripts		
inv	Investment	
oper	Operation and maintenance	
BF	Blast furnace	
HS	Hot stoves	
SF	Shaft furnace	
EAF	Electric arc furnace	
CHP	Combined heat and power	
PP	Pellet plant	
CDQ	Coke dry quenching	
Pel	Pellets	
Pc	Pulverized coal	
Hm	Hot metal	
DRI	Direct reduced iron	
Ls	Liquid steel	
lng	Liquefied natural gas	
El	Electricity	
BFG	Blast furnace top gas	
SFG	Shaft furnace top gas	
H_2recyc	Hydrogen recycling in shaft furnace	
hp	High pressure steam	
mp	Medium pressure steam	
Lp	Low pressure steam	
Dh	District heat	
i	Index for system units	
s	Index for size options	
t	Index for time periods	
T, I, S	denote sets of time periods, system units, and size options	

2. Model description

This section describes the developed optimization model, presenting the objective function and constraints that govern model performance. An integrated steel plant comprises different units contributing to the process of transforming the iron present in iron ore or pellets into steel products. At the start of the considered time horizon, the system consists of the following (main) units: coke plant (CP), air separation unit (ASU),

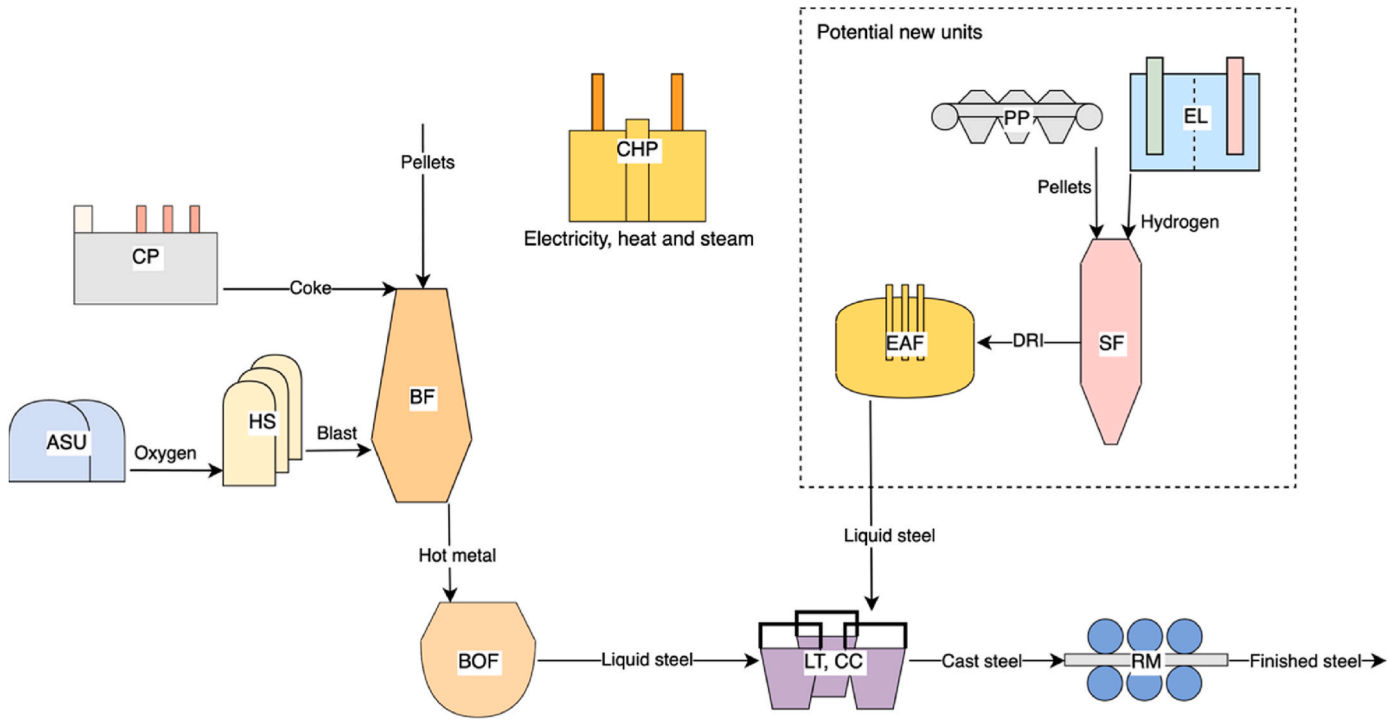

Fig. 1. Simplified schematic overview of the main process units in the steel plant model. A more comprehensive schematic of unit in- and outputs as used in this work is presented in Fig. 8 in Section 3.

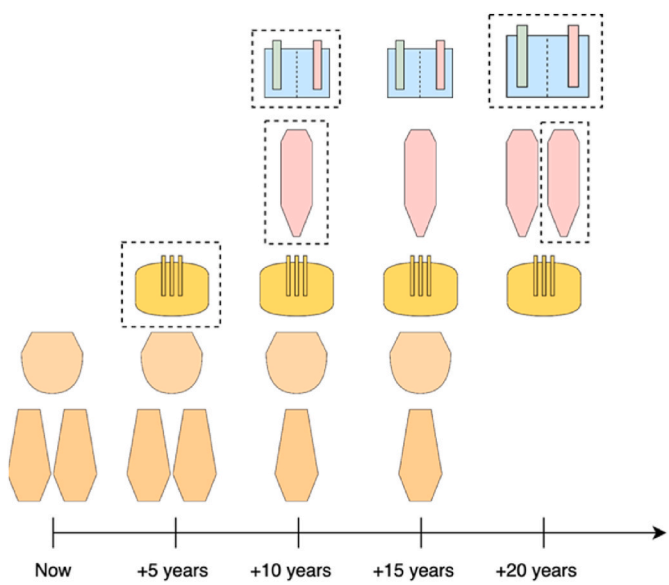

Fig. 2. Schematic example of gradual transition from an initial state to a final state of an integrated steel plant when optimizing investment decisions over a time horizon. Dotted lines around a unit signify a new investment. Detailed example cases are presented in Section 3.

blast furnace (BF) with hot stoves (HS), basic oxygen furnace (BOF), combined heat and power plant (CHP), continuous casting (CC) and rolling mill (RM). Possible new units considered in the transformation to hydrogen-based reduction are: pellet plant (PP), electrolysis unit (EL), shaft furnace (SF) and electric arc furnace (EAF). Fig. 1 shows a schematic of system units and Fig. 8 in Section 3 shows related in- and outputs.

The model is formulated and solved as a mixed-integer non-linear programming (MINLP) problem, searching for optimal values for a set of continuous, integer, and binary variables to minimize an objective function expressing the costs of transition from the present state to a final state, with potential structural changes in the plant setup at discrete intermediate points (Fig. 2). Variable values are constrained by predefined constraints representing physical, practical and logical relations describing the steelworks during a transition period.

2.1. Objective function

The objective function sums either accumulated costs or accumulated CO_2 emissions over the selected time horizon. Costs can be related to investment decisions or to the operation of the system and its units, giving the objective the form

$$\min C = C_{\text{inv}} + C_{\text{oper}} \tag{1}$$

where investment costs are the sum of accumulated investment costs for each new system unit. For a pellet plant and electrolyzers, investment costs are linearly related to their capacities, written in the form (here for the pellet plant)

$$C_{\text{inv,PP}} = \sum_{t \in T} a \times n_{\text{ap}} \times c_{\text{inv,PP},t} \times S_{\text{PP},t} \tag{2}$$

where t is the index for time periods, a is an annuity factor, n_{ap} is the number of years each time period spans, $c_{\text{inv,PP},t}$ is a capacity-dependent cost parameter and $S_{\text{PP},t}$ is the capacity present in time period t. Investment costs for electrolyzers follow an equivalent equation.

Shaft furnaces and EAFs have discrete capacity options, so their investment costs have the form (here for the shaft furnace)

$$C_{\text{inv,SF}} = \sum_{i \in I_{\text{SF}}} \sum_{t \in T} \sum_{s \in S_{\text{SF}}} a \times n_{\text{ap}} \times c_{\text{inv,SF},s,t} \times b_{\text{SF},i,s,t} \tag{3}$$

where i is the index for system units (in this case shaft furnaces in the set I_{SF}), s is the index for size options and $b_{\text{SF},i,s,t}$ is then a binary variable designating the selection of size s for shaft furnace i in time period t. Costs for EAFs follow a similar equation, but binary variables are

Table 1
Blast furnace variable ranges for calculating regression model data points.

Variable	Min. value	Max. value
Hot metal output	50 t/h	180 t/h
Pulverized coal input	0 kg/t_{hm}	250 kg/t_{hm}
Blast oxygen rate	21 %	43 %
Blast temperature	800 °C	1200 °C
DRI input	0 kg/t_{hm}	500 kg/t_{hm}

Table 2
Variable limits used for blast furnace operation.

Variable	Min. value	Max. value
Top gas temperature	115 °C	250 °C
Flame temperature	1850 °C	2300 °C
Blast oxygen rate	21 %	35 %
Blast temperature	800 °C	1200 °C
Hot metal output	80 t/h	160 t/h

Table 3
Shaft furnace variable ranges for calculating regression model data points.

Variable	Min. value	Max. value
Pellet input	50 t/h	300 t/h
Hydrogen input	1600 Nm^3/t_{pel}	1900 Nm^3/t_{pel}
Furnace diameter	3.5 m	5 m
Pellet iron content	64 %	67 %
Hydrogen temperature	1100 °C	1200 °C

replaced with integer variables representing how many furnaces of each size are built.

Blast furnace relining is controlled with binary variables and related costs are formulated as

$$C_{\mathrm{inv,BF}} = \sum_{i \in I_{\mathrm{BF}}} \sum_{t \in T} a \times (n_{\mathrm{p}} - t + 1) \times n_{\mathrm{ap}} \times c_{\mathrm{inv,BF},s,t} \times b_{\mathrm{BFrelin},i,t} \tag{4}$$

where $b_{\mathrm{BFrelin},i,t}$ is a binary variable designating whether blast furnace i has undergone relining in time step t.

Operational costs relate to how the system is functioning in each time step to ensure required steel production rates. Each material flow into the system has a cost coefficient, as listed in Table 5 in Section 3. Costs are also placed on electricity, CO_2 emissions, hydrogen recycling in shaft furnaces and operation of EAFs. Possible profits from selling system outputs such as coke, oxygen and district heat can also be subtracted from the operational costs. Operational costs over the time horizon are summed as

$$\begin{aligned} C_{\mathrm{oper}} = \sum_{t \in T} n_{\mathrm{ap}} \big(& C_{\mathrm{pel},t} + C_{\mathrm{coal},t} + C_{\mathrm{coke},t} + C_{\mathrm{lime},t} + C_{\mathrm{scrap},t} + C_{\mathrm{pc},t} \\ & + C_{\mathrm{lng},t} + C_{\mathrm{O_2},t} + C_{\mathrm{el},t} + C_{\mathrm{H_2recyc},t} + C_{\mathrm{oper,EAF},t} + C_{\mathrm{CO_2},t} - C_{\mathrm{sell},t} \big) \end{aligned} \tag{5}$$

2.2. Constraints

Most of the model constraints represent relations between different mass and energy flows in and out of the system units, mostly either as simple linear relations, or as surrogate models of more detailed and complex models. Except where stated otherwise, these models are similar to those used in Refs. [17–20].

2.2.1. Blast furnaces

Blast furnaces are counter-current reactors in which coke and iron-bearing materials are charged at the top and (possibly oxygen-enriched) hot air, called blast, as well as auxiliary reductants, such as pulverized coal, are injected in the lower part. The iron ore is reduced and finally melted as it descends and is tapped at the bottom as molten iron, called hot metal, along with slag, which holds the liquid by-products. Gases formed in the reactions leave the furnace at the top and are combusted to recover heat in the hot stoves, the coke plant and the CHP plant. A two-zone model of the blast furnace process originally developed by Pettersson and Saxén [17] has earlier been used to optimize the operation of integrated steelworks [18]. This model is in the present work used as a basis for the surrogate model which was built by regression. The reader is referred to Helle [18] for a detailed treatment of the blast furnace model. Other studies have also treated different possible modes of operation included in the model, such as top gas recycling [19] and DRI use [20].

Fig. 3 shows regression model in- and output variables. Note that DRI can be used as a burden material in blast furnaces, e.g., to enhance the production rate or if EAF capacity is limited. Relations between in- and output variables are linear except for the expressions for top gas and

Table 5
Operational cost parameters used in the examples.

Parameter	Cost
Iron ore	80 €/t
Blast furnace pellets	120 €/t
Shaft furnace pellets	140 €/t
Coal	180 €/t
Coke	400 €/t
Pulverized coal	220 €/t
Limestone	30 €/t
LNG	200 €/MWh
DRI	350 €/t
Steel scrap	300 €/t
Oxygen	50 €/kNm^3

Table 6
Investment cost parameters used in the examples.

Parameter	Cost
Electrolyzer	0.4 M€/MW capacity
Pellet plant	1.1 M€/(t/h) capacity
Shaft furnace 150 t/h capacity	300 M€
200 t/h capacity	360 M€
250 t/h capacity	400 M€
EAF 150 t/h capacity	150 M€
200 t/h capacity	180 M€
250 t/h capacity	200 M€
Blast furnace refurbishing	200 M€

Table 4
Example data points of the shaft furnace regression model.

Inputs					Outputs				
$\dot{m}_{\mathrm{pel}}$ [t/h]	$\dot{V}_{\mathrm{H2}}$ [Nm^3/t_{pel}]	d_{SF} [m]	x_{Fe} [−]	T_{H2} [°C]	$\dot{m}_{\mathrm{DRI}}$ [t/h]	x_{SF} [−]	T_{SFG} [°C]	$x_{\mathrm{H2,SFG}}$ [−]	p_{H2} [kPa]
250	1600	4.5	0.65	1150	164.1	0.867	596.7	0.511	279.2
300	1600	4.5	0.65	1150	196.8	0.865	589.4	0.519	314.6
250	1900	4.5	0.65	1150	181.5	1.000	676.7	0.520	302.1
250	1600	5	0.65	1150	165.4	0.870	595.5	0.508	253.7
250	1600	4.5	0.67	1150	166.2	0.833	593.2	0.514	280.7
250	1600	4.5	0.65	1200	170.4	0.971	623.3	0.475	280.2

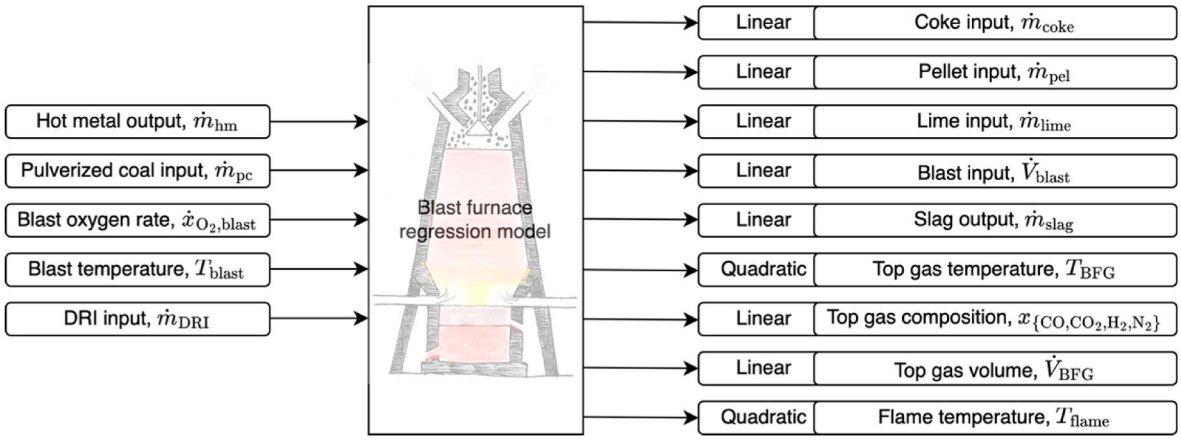

Fig. 3. Blast furnace regression model inputs and outputs.

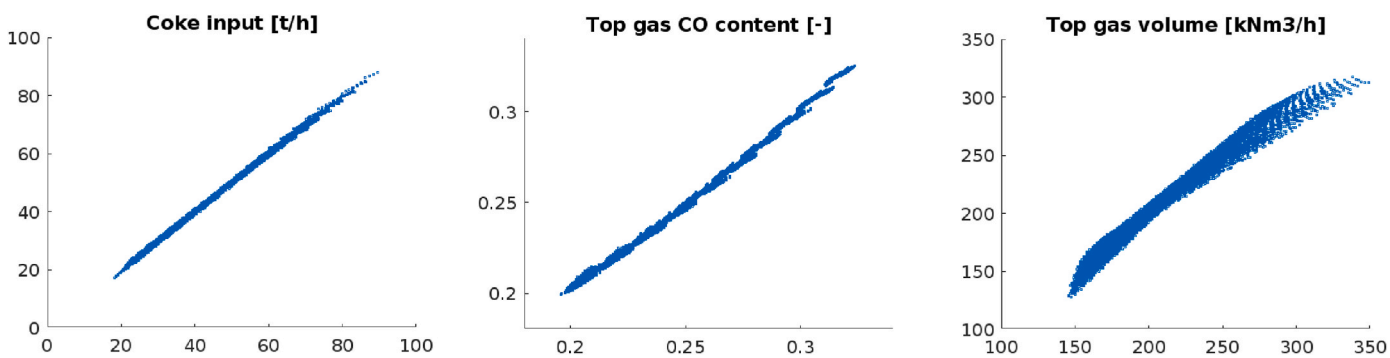

Fig. 4. Examples of linear regression fits of different blast furnace model variables. Values on x-axes are from the original model and y-axes hold corresponding estimates from the linearized models. R^2-values from left to right are 0.99, 0.99 and 0.97.

flame temperatures, which use quadratic relations. To estimate the regression model coefficients, 100 000 data points were generated running the original model with variable value ranges reported in Table 1. Out of these, 15 052 had output values within set variable feasibility limits and were used to determine regression model coefficients. Most R^2-values for the resulting approximations were above 0.95, but linear approximations for flame and top gas temperatures had R^2-values below 0.8, so these were additionally approximated with quadratic functions, giving R^2-values above 0.95. Fig. 4 shows three examples of acceptable linear approximation fits, with coke input and top gas CO content fitting very well. The top gas volume shows overestimated values in both extremes, but the regression is performed over a wider interval of input values for the hot metal and blast oxygen rates than the optimization model will allow. Within variable limits of the optimization model, the regression model is deemed to be adequate. Fig. 5 shows both the excessively widespread linear approximation fits of the top gas and flame temperatures, and the better quadratic approximation fits.

In addition to the variables above, scrap input, required steam input and district heat output are defined as proportional to hot metal output. E.g., in the example cases in this article the value 20 kg/thm was used for the scrap rate. Along with these relations between inputs and outputs, constraints ensuring proper function of the blast furnace model are defined. While existence of blast furnace i in time step t is represented by binary variables $y_{i,t}$, binary variables $b_{i,t}$ tell whether blast furnaces are in use in a time period or not. These variables are used, e.g., to define a minimum hot metal output in the case a blast furnace is in operation as

$$\dot{m}_{\mathrm{hm},i,t} \geq b_{i,t}\dot{m}_{\mathrm{hm,BF,max}} \quad i \in I_{\mathrm{BF}}, t \in T \tag{6}$$

$$b_{i,t} \leq y_{i,t} \quad i \in I_{\mathrm{BF}}, t \in T \tag{7}$$

Generally, blast furnace variable limits, as listed in Table 2, are implemented as constraints that are active only if the blast furnace is in operation, using binary variables $b_{i,t}$.

2.2.2. Hot stoves

Air and possible added oxygen injected into blast furnaces are preheated using blast furnace gas in sets of regenerative heat exchangers called hot stoves. Air and oxygen are compressed and blown through the hot stoves before being led to the blast furnace tuyeres. The original blast furnace model also includes hot stoves models, from which relations for compressor electricity demand, heat transfer in the stove, hot gas temperature and blast furnace gas demand were simplified through linear regression, resulting in the following constraints for each set of stoves:

$$P_{\mathrm{HS},i,t} = K_{\mathrm{HS,P,air}}\dot{V}_{\mathrm{air},i,t} \quad i \in I_{\mathrm{HS}}, t \in T \tag{8}$$

$$\dot{Q}_{\mathrm{HS},i,t} = K_{\mathrm{HS,Q,0}}y_{i,t} + K_{\mathrm{HS,Q,1}}\dot{V}_{\mathrm{air},i,t} + K_{\mathrm{HS,Q,2}}T_{\mathrm{blast}} \quad i \in I_{\mathrm{HS}}, t \in T \tag{9}$$

$$\begin{aligned} T_{\mathrm{gas,HS},i,t} = {} & K_{\mathrm{HS,T,0}}y_{i,t} + K_{\mathrm{HS,T,1}}\dot{V}_{\mathrm{air},i,t} + K_{\mathrm{HS,T,2}}T_{\mathrm{blast},i,t} + K_{\mathrm{HS,T,3}}\dot{Q}_{\mathrm{HS},i,t} \\ & + K_{\mathrm{HS,T,4}}x_{\mathrm{CO},i,t} + K_{\mathrm{HS,T,5}}x_{\mathrm{CO_2},i,t} + K_{\mathrm{HS,T,6}}x_{\mathrm{N_2},i,t} \quad i \\ & \in I_{\mathrm{HS}}, t \in T \end{aligned} \tag{10}$$

$$\begin{aligned} \dot{V}_{\mathrm{BFG,HS},i,t} = {} & K_{\mathrm{HS,V,0}}y_{i,t} + K_{\mathrm{HS,T,1}}\dot{V}_{\mathrm{air},i,t} + K_{\mathrm{HS,T,2}}T_{\mathrm{blast},i,t} + K_{\mathrm{HS,T,3}}\dot{Q}_{\mathrm{HS},i,t} \\ & + K_{\mathrm{HS,T,4}}x_{\mathrm{CO},i,t} + K_{\mathrm{HS,T,5}}x_{\mathrm{CO_2},i,t} + K_{\mathrm{HS,T,6}}x_{\mathrm{N_2},i,t} + K_{\mathrm{HS,T,7}}T_{\mathrm{gas,HS},i,t} \quad i \\ & \in I_{\mathrm{HS}}, t \in T \end{aligned} \tag{11}$$

Additionally, the blast oxygen content is described with the nonlinear constraint

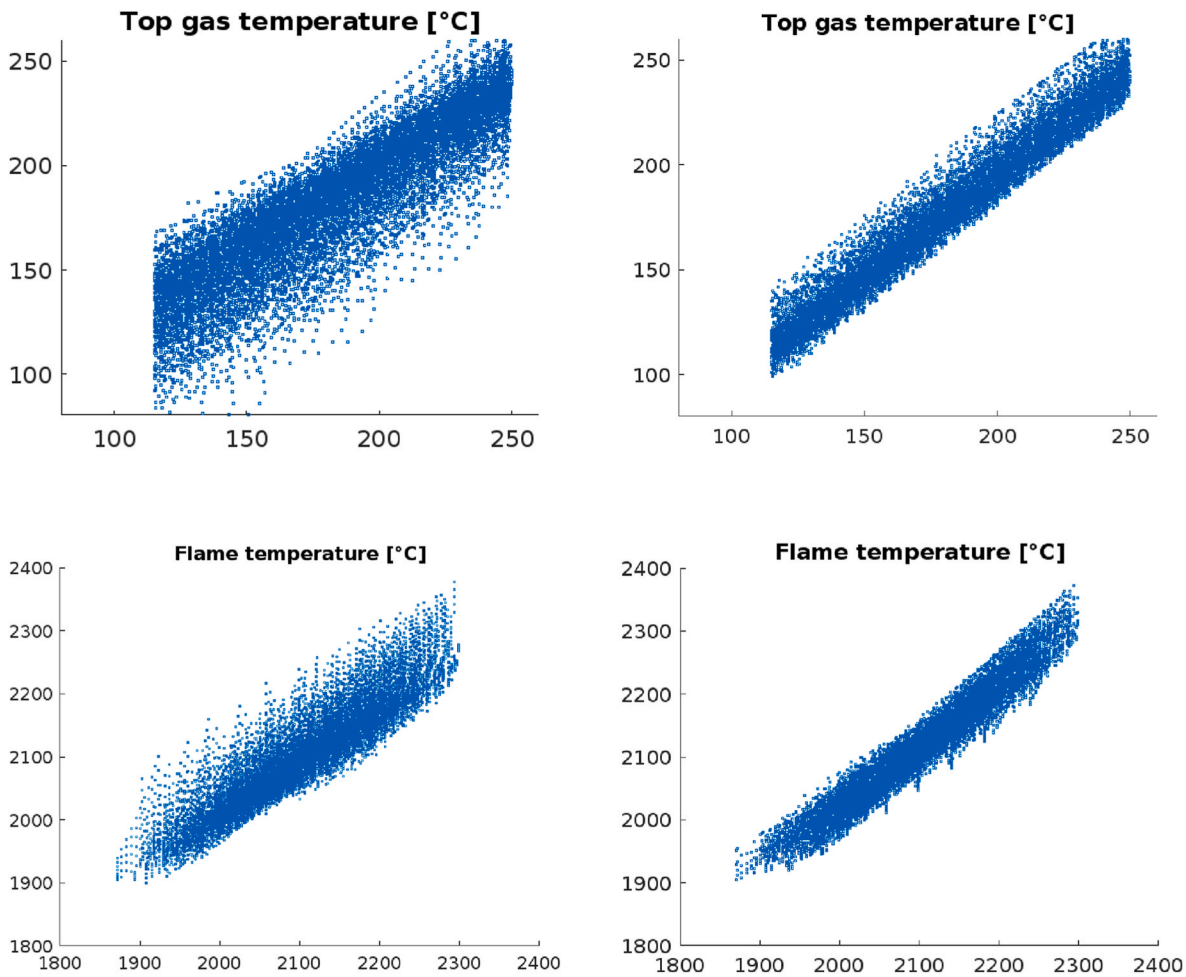

Fig. 5. Regression model fits for the top gas and flame temperatures. Figures on the left show the linear fits (R^2-values 0.84 and 0.87) and figures on the right show the improved quadratic fits (R2-values 0.99 and 0.99).

$$x_{O_2,i,t}\dot{V}_{\text{blast},i,t} = \dot{V}_{O_2,i,t} + 0.21\dot{V}_{\text{air},i,t} \quad i \in I_{\text{HS}}, t \in T \tag{12}$$

2.2.3. Combined heat and power plant

The CHP plant as part of a steel plant model is based on descriptions by Pikkuaho [21]. The model mainly relates inputs of energy as fuels and process gases to outputs of heat, electricity and steam. Possible inputs in the present model setup are coke oven gas, blast furnace gas, basic oxygen furnace gas and LNG. Additionally, the power plant gets a steam input from coke dry quenching in the coke plant. Process steam for the steelworks can be tapped from the power plant turbine at high, medium or low pressures. The energy available for use is

$$\dot{Q}_{\text{tot},t} = \dot{E}_{\text{CHP,in},t} - 0.9\dot{V}_{\text{flue},i,t}h_{\text{flue}} \quad t \in T \tag{13}$$

where the value for the flue gas specific enthalpy h_{flue} is approximated from output data from the steelworks model by Helle [18] as 0.27 MJ/kNm^3. The total mass of available steam is then calculated as

$$\dot{m}_{\text{steam},t} = \frac{\dot{Q}_{\text{tot},t} + H_{\text{CDQ},t}}{h_{\text{hp}} - h_0} \quad t \in T \tag{14}$$

where $h_{\text{hp}} = 3.46$MJ/kg is the specific enthalpy of steam at 525 °C and 82 bar and $h_0 = 0.21$MJ/kg is the specific enthalpy of outlet water at 50 °C and 0.2 bar. Blast furnaces, the basic oxygen furnace and rolling mills have steam requirements depending on their output rates, and these must be covered in the model. Half of the total steam requirement is assumed to be high-pressure steam, and half is medium-pressure steam. The power output is the sum of power taken at the three pressure levels

$$P_{\text{CHP,tot},t} = \eta\left(P_{\text{hp},t} + P_{\text{mp},t} + P_{\text{lp},t}\right) \quad t \in T \tag{15}$$

$$P_{\text{hp},t} = \dot{m}_{\text{steam},t}\left(h_{\text{hp}} - h_{\text{mp}}\right) \quad t \in T \tag{16}$$

$$\dot{m}_{\text{steam,mp},t} = \dot{m}_{\text{steam},t} - 0.5\dot{m}_{\text{steam,req},t} \quad t \in T \tag{17}$$

$$P_{\text{mp},t} = \dot{m}_{\text{steam,mp},t}\left(h_{\text{mp}} - h_{\text{lp}}\right) \quad t \in T \tag{18}$$

$$\dot{m}_{\text{steam,lp},t} = \dot{m}_{\text{steam,mp},t} - 0.5\dot{m}_{\text{steam,req},t} - \dot{m}_{\text{steam,dh},t} \quad t \in T \tag{19}$$

$$P_{\text{lp},t} = \dot{m}_{\text{steam,lp},t}\left(h_{\text{lp}} - h_{\text{out}}\right) \quad t \in T \tag{20}$$

where η is the overall efficiency, $\dot{m}_{\text{steam,req},t}$ is the total steam requirement at the steelworks and $\dot{m}_{\text{steam,dh},t}$ is steam used to provide district heat. A binary variable $b_{\text{CHP},t}$ indicates whether the CHP plant is in use in a time step. If it is operating, the total flow of steam $\dot{m}_{\text{steam},t}$ needs to be between 40 kg/s and 110 kg/s for the turbine to function reliably.

2.2.4. Air separation units

Air separation units produce pure oxygen from air through cryogenic separation, which requires electricity. These are simply modelled by a linear relation between the oxygen output and the required amount of electricity, e.g., 0.426 MW per every kNm^3/h increase in oxygen output as used in the example cases in this article.

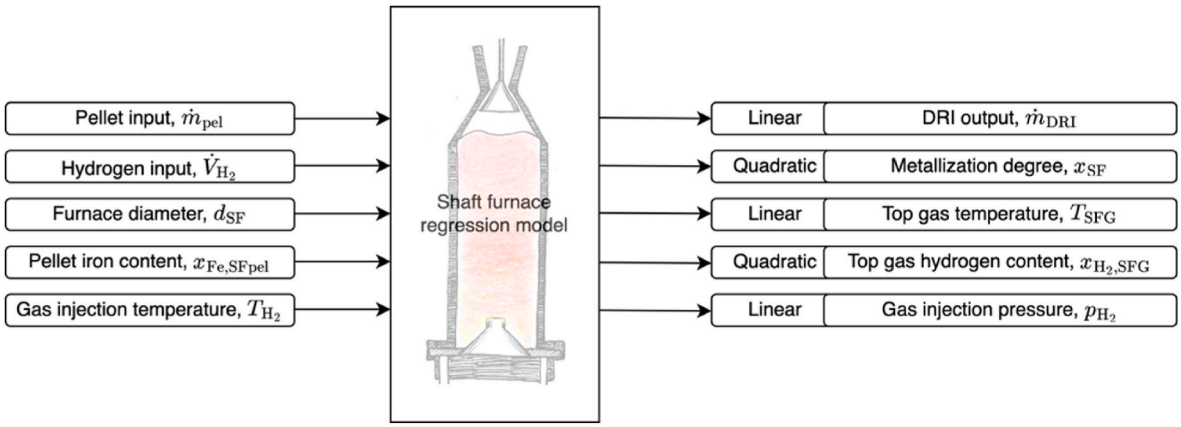

Fig. 6. Inputs and outputs of the shaft furnace regression model.

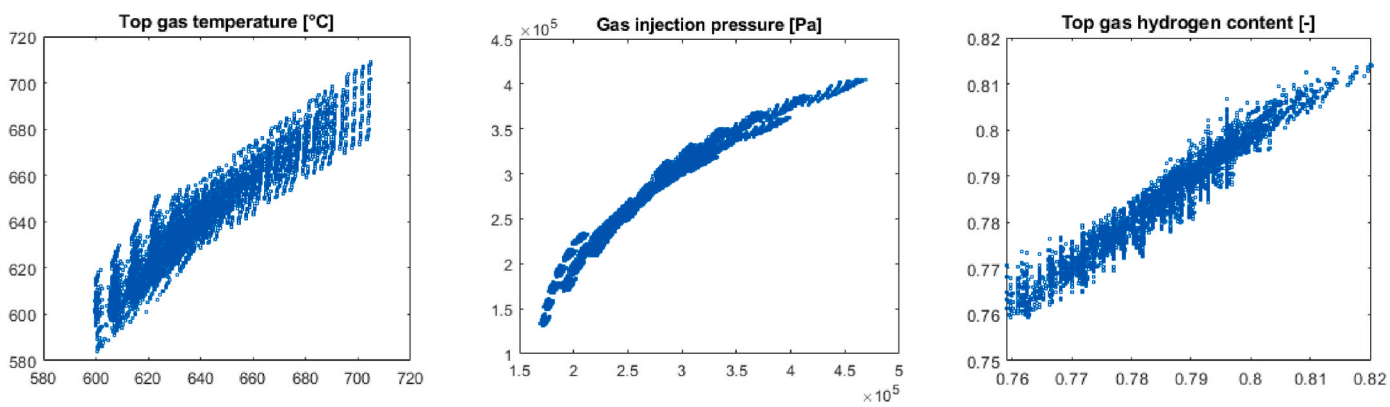

Fig. 7. Examples of regression model fits of different shaft furnace model variables. Values on x-axes are from the original model and y-axes hold corresponding estimates from the regression models. Top gas temperature and gas injection pressure models are linear, and the top gas hydrogen content model is quadratic. R^2-values from left to right are 0.90, 0.94 and 0.93.

2.2.5. Basic oxygen furnace

In the BF-BOF route, basic oxygen furnaces primarily convert hot metal to liquid steel. To some extent, hot metal can be replaced by a cold charge of scrap and/or DRI [22]. In this model, it is assumed that this cold charge can be maximally 25 % of the hot metal charge. A rate for the conversion of hot metal is calculated from a carbon balance as

$$x_{ls} = \left(1 - X_{BOF,loss}\right)\frac{1 - X_{C,hm}}{1 - X_{C,ls}} \tag{21}$$

where $X_{BOF,loss}$ is an assumed loss in the process, with $X_{C,hm}$ and $X_{C,ls}$ being the carbon content of the hot metal and liquid steel, respectively. Scrap and DRI are assumed to be fully converted to liquid steel. With another conversion loss in continuous casting $X_{CC,loss}$, the output of steel slabs is calculated as

$$\dot{m}_{slab,t} = \left(1 - X_{CC,loss}\right)\left(x_{ls}\dot{m}_{hm,t} + \dot{m}_{scrap,t} + \dot{m}_{DRI,t}\right) \quad t \in T \tag{22}$$

Oxygen input rates and gas output rates are expressed as linear functions of iron inputs, while lime and steam input rates, electricity demand, and heat output for district heat are linear functions of the steel output.

2.2.6. Coke plant

Coke for the blast furnaces can be from a coke plant at the steelworks or externally bought. Coke and coke oven gas outputs are linear functions of coal input. The coke ovens use blast furnace gas as an energy source and the required gas input is also a linear function of the coke output, as is electricity demand and steam output from coke dry quenching. Coke from the coke plant can also be sold outside the system, the profits of which may be subtracted from total system operational costs if it is considered in an analysis.

2.2.7. Rolling mills

After continuous casting, the steel is processed in rolling mills. A prespecified rate of material loss $X_{RM,loss}$ is assumed at this stage. The process uses coke oven gas and/or LNG as an energy source, modelled as a linear function of the steel output. The process also requires electricity, steam and oxygen, and outputs heat for district heating and scrap that can be reused on site.

2.2.8. Electrolyzers

The transition to hydrogen-based reduction of iron requires a source of hydrogen. This model gives the option of investing in electrolysis units at the steelworks. Modelling-wise, the most important parameter is the efficiency, i.e., the electricity needed per volume unit of hydrogen produced. Values reported for this parameter have been, e.g., 4.1 MWh/kNm^3 [9] and 4.2–4.8 MWh/kNm^3 [23] for commercial alkaline electrolyzers. Part of the by-product oxygen can also be utilized at the steelworks or exported outside the system. Large amounts of heat at temperatures around 70 °C are also generated in the electrolysis process [24], but this heat is not considered in the present model.

2.2.9. Pellet plant

It is assumed that iron pellets for the DR process need to be of a different quality than pellets used in blast furnaces. Shaft furnace pellets can either be externally bought or produced in a pellet plant which is

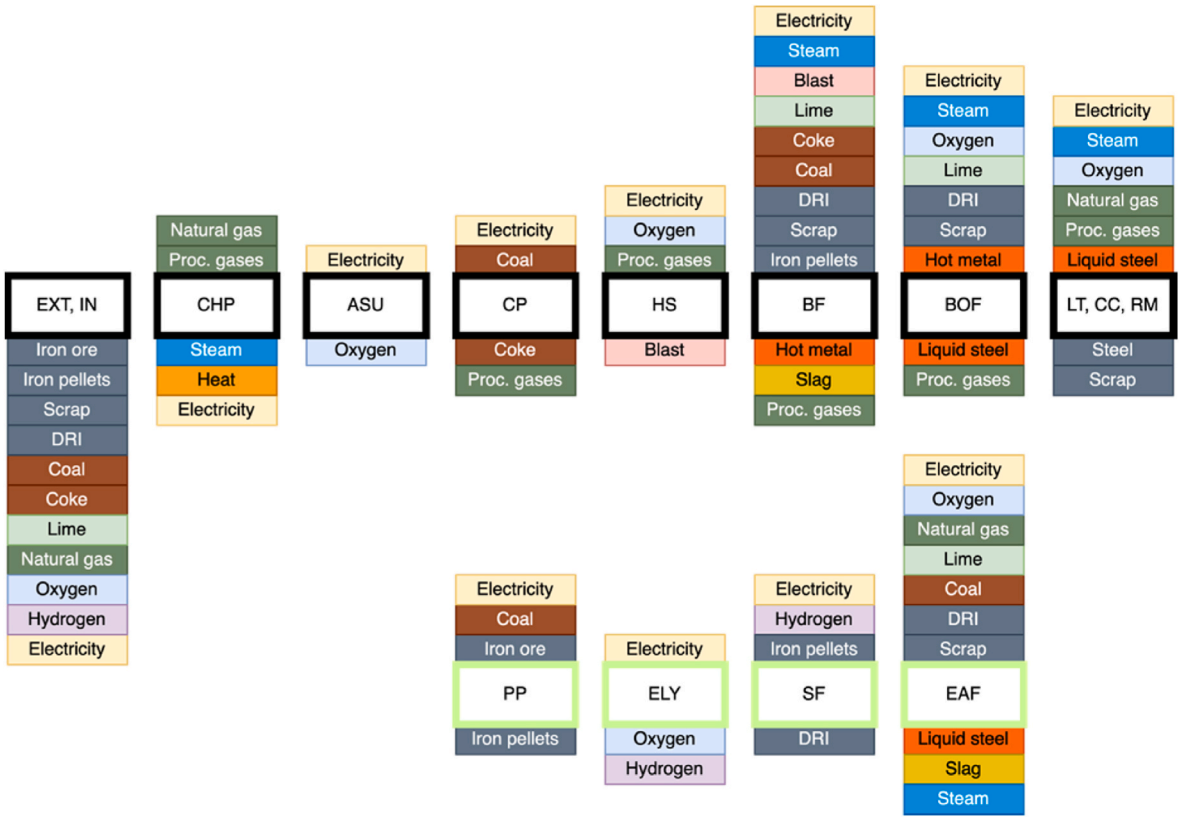

Fig. 8. In- and outputs of system units in the model. Inputs are above the units and outputs below. Abbreviations: EXT, IN – External imports; CHP – Combined heat and power plant; ASU – Air separation unit; CP – Coke plant; HS – Hot stoves; BF – Blast furnace; BOF – Basic oxygen furnace; LT, CC, RM – Ladle treatment, continuous casting and rolling mills; PP – Pellet plant; ELY – Electrolyzer; SF – Shaft furnace; EAF – Electric arc furnace.

among the new possible investments in the model. The pellet plant model follows linear relations between pellet output and iron ore, coal and electricity requirements. It is also assumed that only one pellet plant can be built within the time horizon. Plant capacity is thus set once it has been built, by the constraint

$$S_{\mathrm{PP},t} \leq S_{\mathrm{PP},t-1} + S_{\mathrm{PP,max}}\left(1 - y_{\mathrm{PP},t-1}\right) \quad t > 1 \tag{23}$$

2.2.10. Shaft furnaces

In the H2-SF route the hydrogen-based reduction of iron takes place in shaft furnaces where pellets are charged at the top and hydrogen gas enters in the lower part. The reduced iron is extracted at the bottom while top gas largely consisting of water and unreacted hydrogen exits at the top. Shao et al. [8] have studied the process with a one-dimensional model that considers the heat and mass transfer and main chemical reactions occurring in the furnace. Using data from this model as a base, a regression model was created similarly as with the blast furnace model. In- and output variables for the regression model are shown in Fig. 6. Input variable values were distributed between the intervals in Table 3 to create 5760 data points, of which 4933 had metallization rates above 0.85, which was chosen as a lower limit as a certain level of metallization is needed for further processing in the EAF [8]. These feasible data points were used to approximate relations between input and output variables, with linear functions for the DRI input, top gas temperature and gas injection pressure, and quadratic functions for the metallization degree and top gas hydrogen content. Fig. 7 shows examples of regression model fits and Table 4 shows some example regression data points, altering the input variable values one at a time.

As the metallization degree cannot exceed 100 %, an additional binary variable b_x designates whether the regression function exceeds 1, keeping the value within the limit with the equations

$$x_{\mathrm{SF,calc},i,t} \leq 1 + Mb_{\mathrm{x},i,t} \quad i \in I_{\mathrm{SF}},\ t \in T \tag{24}$$

$$x_{\mathrm{SF},i,t} \leq x_{\mathrm{SF,calc},i,t} + Mb_{\mathrm{x},i,t} \quad i \in I_{\mathrm{SF}},\ t \in T \tag{25}$$

$$x_{\mathrm{SF},i,t} \geq x_{\mathrm{SF,calc},i,t} - Mb_{\mathrm{x},i,t} \quad i \in I_{\mathrm{SF}},\ t \in T \tag{26}$$

$$x_{\mathrm{SF},i,t} \leq 1 + M\left(1 - b_{\mathrm{x},i,t}\right) \quad i \in I_{\mathrm{SF}},\ t \in T \tag{27}$$

$$x_{\mathrm{SF},i,t} \geq 1 - M\left(1 - b_{\mathrm{x},i,t}\right) \quad i \in I_{\mathrm{SF}},\ t \in T \tag{28}$$

$$b_{\mathrm{x},i,t} \leq y_{i,t} \quad i \in I_{\mathrm{SF}},\ t \in T \tag{29}$$

where $x_{\mathrm{SF,calc},i,t}$ is the value for the metallization degree from the regression model and $x_{\mathrm{SF},i,t}$ is the value used in the optimization model.

Shaft furnace diameters represent furnace dimensions overall. When calculating data points for the regression model, the furnace height was also varied in proportion with the diameter. This simplified treatment of furnace scaling differs from a more detailed scale-up, but was deemed adequate for this regression model. With development of more detailed shaft furnace models, also the regression model variables need to be reconsidered. Furnace geometry is to remain unchanged once a furnace is built, which is ensured with the constrains

$$d_{i,t} \leq d_{i,t-1} + d_{\mathrm{SF,max}}\left(1 - y_{i,t-1}\right) \quad i \in I_{\mathrm{SF}},\ t > 1 \tag{30}$$

$$d_{i,t} \geq d_{i,t-1} - d_{\mathrm{SF,max}}\left(1 - y_{i,t-1}\right) \quad i \in I_{\mathrm{SF}},\ t > 1 \tag{31}$$

Additional variables are used to allow situations where a shaft furnace has been built but is not in use.

Studies by Shao et al. [8] indicate that shaft furnace top gas can contain large amounts of unreacted hydrogen that should preferably be

recycled, and top gas recycling is also assumed, e.g., in studies by Vogl et al. [9] and Li et al. [25]. In the present model, rates of recycled and fresh hydrogen are constrained by the equations

$$\dot{V}_{H_2,i,t} + \dot{V}_{H_2,\mathrm{recyc},i,t} \geq \lambda_{\min} V_{H_2,\min} \dot{m}_{\mathrm{DRI},i,t} \quad i \in I_{\mathrm{SF}},\ t \in T \tag{32}$$

$$\dot{V}_{H_2,i,t} \geq \lambda_{\min,\mathrm{fresh}} V_{H_2,\min} \dot{m}_{\mathrm{DRI},i,t} \quad i \in I_{\mathrm{SF}},\ t \in T \tag{33}$$

$$\dot{V}_{H_2,\mathrm{recyc},i,t} \leq X_{\mathrm{recyc,max}} x_{H_2,\mathrm{SFG},i,t} \left(\dot{V}_{H_2,i,t} + \dot{V}_{H_2,\mathrm{recyc},i,t}\right) \quad i \in I_{\mathrm{SF}},\ t \in T \tag{34}$$

where $\lambda_{\min}$ expresses the amount of hydrogen required for the process, with $\lambda_{\min} = 1$ giving the value $V_{H_2,\min}$, which is the theoretically minimum amount required per ton DRI produced. In the regression model data points, the smallest values for $\lambda_{\min}$ were about 3.6, so this value was used in the optimization model. The smallest rate of hydrogen that needs to be fresh hydrogen, $\lambda_{\min,\mathrm{fresh}}$, was set to be 1.5, based on the required hydrogen rate used by Vogl et al. [9]. The maximum rate of hydrogen recyclable from the top gas was given the value $X_{\mathrm{recyc,max}} = 0.9$. A cost is placed on recycling hydrogen, reflecting costs of top gas processing. Heating of the hydrogen to the desired injection temperature T_{H_2} requires energy, which is here treated as an additional electricity requirement.

Shaft furnace capacities are selected from discrete options. In the optimization cases in this paper maximum DRI output options were 150 t/h, 200 t/h or 250 t/h, for which three binary variables b_{small}, b_{medium} and b_{large} were designated for each possible shaft furnace. One size option is chosen for each built shaft furnace with the constraint

$$b_{\mathrm{small},i,t} + b_{\mathrm{medium},i,t} + b_{\mathrm{large},i,t} \leq y_{i,t} \quad i \in I_{\mathrm{SF}},\ t \in T \tag{35}$$

and the corresponding maximum capacity is ensured with the constraints

$$S_{\max,i,t} = S_{\mathrm{small,SF}} b_{\mathrm{small},i,t} + S_{\mathrm{medium,SF}} b_{\mathrm{medium},i,t} + S_{\mathrm{large,SF}} b_{\mathrm{large},i,t} \quad i \in I_{\mathrm{SF}},\ t \in T \tag{36}$$

$$\dot{m}_{\mathrm{DRI},i,t} \leq S_{\max,i,t} \quad i \in I_{\mathrm{SF}},\ t \in T \tag{37}$$

Shaft furnace electricity requirements are calculated as a linear function of DRI output and hydrogen gas input temperature.

2.2.11. Electric arc furnaces

EAFs commonly melt recycled steel scrap, but in the H2-SF route they are also fed DRI from shaft furnaces. Effects of different DRI-to-scrap ratios in EAFs have been studied by Kirschen et al. [26]. In the present model, the ratio of DRI per the total input is defined as a variable $x_{\mathrm{DRI},t}$, determined by the constraint

$$x_{\mathrm{DRI},t} \dot{m}_{\mathrm{DRI},t} + x_{\mathrm{DRI},t} \dot{m}_{\mathrm{scrap},t} - \dot{m}_{\mathrm{DRI},t} = 0 \quad t \in T \tag{38}$$

This ratio affects the electricity requirement and metal yield of the furnaces according to

$$P_t = \left(K_{0,\mathrm{P}} + K_{1,p} x_{\mathrm{DRI},t}\right) \dot{m}_{\mathrm{ls},t} \quad t \in T \tag{39}$$

$$\dot{m}_{\mathrm{ls},t} = \left(K_{0,\mathrm{x}} + K_{1,x} x_{\mathrm{DRI},t}\right) \left(\dot{m}_{\mathrm{DRI},t} + \dot{m}_{\mathrm{scrap},t}\right) \quad t \in T \tag{40}$$

Carbon, lime and oxygen are usually added to achieve desired properties of steel and slag in the EAF [27]. A more detailed mass balance presented by Hay et al. [27] also considers inputs representing electrode consumption, furnace refractory and a small amount of natural gas injection, but these are not considered in the present model due to their relatively small quantities. In the model, flow rates of carbon, lime and oxygen are proportional to the output of liquid steel and part of the excess heat from a furnace can be used for district heating or to produce process steam.

As with shaft furnaces, three maximum capacity options are given for EAFs: 150 t/h, 200 t/h and 250 t/h. Integer variables represent how many of each size are built. EAFs are treated as one unit, the capacity of which is expressed as

$$\dot{m}_{\mathrm{ls},t} \leq S_{\mathrm{small,EAF}} n_{\mathrm{small},t} + S_{\mathrm{medium,EAF}} n_{\mathrm{medium},t} + S_{\mathrm{large,EAF}} n_{\mathrm{large},t} \quad t \in T \tag{41}$$

2.3. CO_2 emissions

Accumulated system CO_2 emissions are evaluated for the optimization time horizon. First, a carbon balance is considered, with any carbon entering and not exiting the system as part of steel or exported coke assumed to contribute to direct CO_2 emissions [18]. A cost is placed on these emissions, in line with existing carbon credit markets. Additionally, when minimizing emissions, indirect upstream emissions related to, e.g., electricity from the grid are included in the objective function to account for emissions caused by decisions made in the solutions and to have a fair comparison of the different options and input parameters.

2.4. Model implementation

The described model was programmed in Python using the Pyomo optimization modelling framework [28] as a mixed-integer quadratically constrained programming problem solved with Gurobi 10.0 [29]. Most of the problem instances were solved quickly on a laptop computer with a 2.7 GHz Dual-Core Intel Core i5 processor and 8 GB RAM, with solution times usually between a few seconds to a few minutes, as long as the number of time periods was five or less. Increasing the time steps greatly increases the required computational time and solving the model with more than seven time periods seems unfeasibly time consuming in its current formulation. This necessitates balancing the time resolution and the length of the optimized timeframe when planning optimization cases and can make it difficult to identify optimal solutions in situations where short investment intervals would be beneficial. The examples in the next section were calculated with five time periods, each representing five years, giving a total time horizon of 25 years.

3. Example cases

To demonstrate the model, three example cases and their solutions are next described. The cases involve an integrated steel plant, initially with two blast furnaces and a basic oxygen furnace. The steel plant has been in operation for decades, and currently one blast furnace is planned for relining or decommissioning in 10 years, and the other in 20 years. All other units are taken to have a life length of 25 years or more. Processes are integrated, with process gases being utilized across different units as an energy source. Fig. 8 presents a schematic of units with their in- and outputs, where the upper row are the existing ones and the bottom row represents new possible unit processes. The steel plant is expected to produce steel at a rate of 260 t/h, and this is kept constant throughout the time horizon.

The three cases optimize projected future investments and operation of the example steel plant with three different assumptions to compare how constraints and parameter values affect optimal system configurations. In Case 1, transition to the H2-DR route is enforced by not giving the option of relining the blast furnaces or importing scrap for the EAFs. This represents a situation where the future strategy has already been decided but the path of implementing it during upcoming years has not yet been decided. In Case 2, the alternatives of blast furnace relining and importing scrap for EAF operation are added. In contrast with Case 1, a future strategy has not been decided, and it might include any mix of BF-BOF, H2-DR or EAFs charged with recycled scrap. Case 3 again enforces transition to the H2-DR route as in Case 1, but test how higher costs on CO_2 emissions affect the optimization outcome.

Table 5 lists operational cost parameters in the example cases: cost parameters were selected based on a comparison between values presented by Helle [18], OECD [30], Bhaskar et al. [10] and Vogl et al. [9], considering the fluctuations in raw material costs presented by OECD [30]. Shaft furnace pellet costs were estimated as slightly higher than

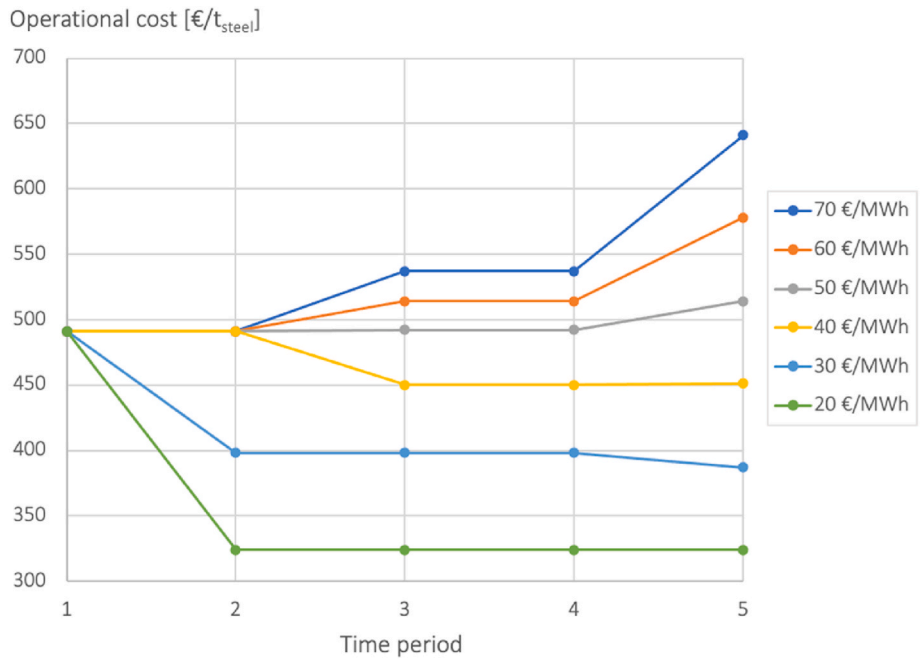

Fig. 9. Evolution of operational costs when minimizing accumulated costs in Case 1.

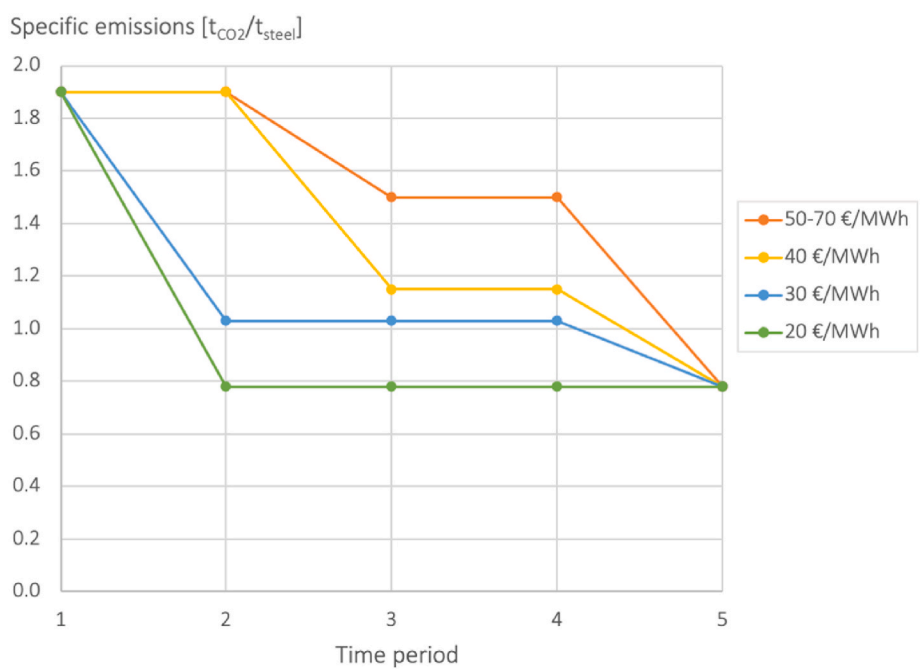

Fig. 10. Evolution of specific emissions when minimizing accumulated costs in Case 1.

blast furnace pellets. Electrolyzer investment costs are based on IRENA [31], selecting a value between cost estimates for 2020 and 2050. Additionally, operating costs were placed on hydrogen recycling in the shaft furnace (10 €/kNm^3) and EAF operation (8 €/t_{steel}). Costs were also assigned to CO_2 emissions, defined as 80 €/t_{CO2} in Cases 1 and 2, and 150 €/t_{CO2} in Case 3. Profits from selling coke, oxygen and district heat from the steelworks were not included in these case studies. Raw material prices can vary greatly over time [30], and uncertainties in costs over a longer time horizon should be considered in more thorough analyses but were left out in these simple examples.

Electrolyzer efficiency was fixed at 4.1 MWh/kNm^3, although, e.g., Vartiainen et al. [32] assume a steady annual increase in efficiency. Electrolyzer investments were considered to include small storage capacities of produced hydrogen, but not large storage allowing for dynamic operation.

For the sake of demonstrating model functionality, the costs were kept constant in the example cases. In reality, costs would vary from case to case and over the time horizon. A more thorough analysis, beyond the scope of this article, would consider different projections and ranges of cost and technology developments, which can easily be implemented in the model by adjusting the parameters.

With the described cost structure, the system was optimized for a time horizon of 25 years, with investment decisions possible every 5 years.

Table 7
Optimal system configuration in Case 1 for 40 €/MWh electricity cost. Top half of rows shows maximum capacities and hourly outputs, bottom half shows hourly outputs.

Unit	T1	T2	T3	T4	T5
	2 x 160 t/h 252 t/h	2 x 160 t/h 252 t/h	160 t/h 95 t/h	160 t/h 95 t/h	
			905 MW 181 kNm^3/h	905 MW 181 kNm^3/h	1451 MW 290 kNm^3/h
			200 t/h 200 t/h	200 t/h 200 t/h	200 + 150 t/h 321 t/h
			200 t/h 172 t/h	200 t/h 172 t/h	200 + 150 t/h 277 t/h
			444 t/h 277 t/h	444 t/h 277 t/h	444 t/h 444 t/h
	277 t/h	277 t/h	104 t/h	104 t/h	
	105 t/h	107 t/h	38 t/h	38 t/h	
	83 MW_{el}	69 MW_{el}	43 MW_{el}	43 MW_{el}	
	14 kNm^3/h	12 kNm^3/h			
0	260 t/h	260 t/h	260 t/h	260 t/h	260 t/h

3.1. Grid emission intensities

Grid emission intensities were varied to compare emissions from the BF-BOF route and the electricity-intensive H2-SF route. Assuming 100 % DRI charge to EAFs and minimizing total accumulated system emissions for the time horizon, model solutions favored quick transition to the H2-SF route when grid emission intensities were below about 0.2 t_{CO2}/MWh. Values between 0.2 and 0.3 t_{CO2}/MWh gave solutions featuring both routes, and above 0.3 t_{CO2}/MWh solutions completely favored the BF-BOF route. Thus, the break-even suggested here is considerably lower than the value 0.532 t_{CO2}/MWh suggested by Vogl et al. [9].

In the example cases presented below, grid emission intensities were kept constant at 0.089 t_{CO2}/MWh, an average value reported for Finnish grid electricity in 2018–2022 [33], although these emissions could decrease during upcoming years. Electricity costs were varied between 20 and 70 €/MWh to see how this affects the solutions.

3.2. Case 1 – forced transition

First, total accumulated costs were minimized for a scenario where a forced transition to the H2-DR route was imposed by banning blast furnace relining and scrap inputs to EAFs. Thus, one of the blast furnaces must be blown out after ten years, i.e., two sub-periods. This resulted in the evolution of operational costs and specific emissions shown in Figs. 9 and 10. Reported emissions values include emissions from the processes at the steel plant as well as upstream emissions related to raw materials and electricity. Emissions related to steel scrap bought from the market were based on Van der Voet et al. [34]. Investment costs in the different solutions varied from 6 % of the total costs with 70 €/MWh electricity cost to 15.6 % of total costs with 20 €/MWh. A breakdown of total accumulated costs over the modelled time horizon is shown in Fig. 12 (see Table 6).

Initially, in the first time period, all the steel is produced via the BF-BOF route, with operational costs of 491 €/t_{steel} and specific emissions of 1.90 t_{CO2}/t_{steel}. These specific emissions largely agree with values reported by, e.g., Perpiñán et al. [35] and the World Steel Association [36]. Recent prices for flat steel products have ranged from about 500 USD/t in 2016 to about 1000 USD/t in 2022 [30]. For electricity costs of 50 €/MWh or above, operational costs are increasing, while they are decreasing with lower electricity costs. This is in line with results of, e.g., Vogl et al. [9] who estimated that the H2-DR route could be competitive with the BF-BOF route with electricity prices of 40 €/MWh or lower. Changes in costs and emissions in each time period are directly related to changes in system configuration towards the H2-DR route. Most solutions end at the same configuration, where the two blast furnaces eventually are replaced with two shaft furnaces, with capacities 200 t/h and 150 t/h, and two EAFs, also 200 t/h and 150 t/h. The only exception is the solution for 20 €/MWh electricity cost, which manages with two 150 t/h EAFs. System operation may also differ between similar solutions, as, e.g., the solution with 30 €/MWh features a DRI input to the blast furnace in time periods 3 and 4. Carbon intensity of the steel in time step 5 is 0.78 t_{CO2}/t_{steel}. An example of how the system configuration develops with electricity costs 40 €/MWh is given in Table 7. Additionally, the evolution of electricity used in the same example case solution is shown in Fig. 13.

With electricity costs of 40 €/MWh or higher, one blast furnace is replaced with a shaft furnace and an EAF at the point of decommissioning

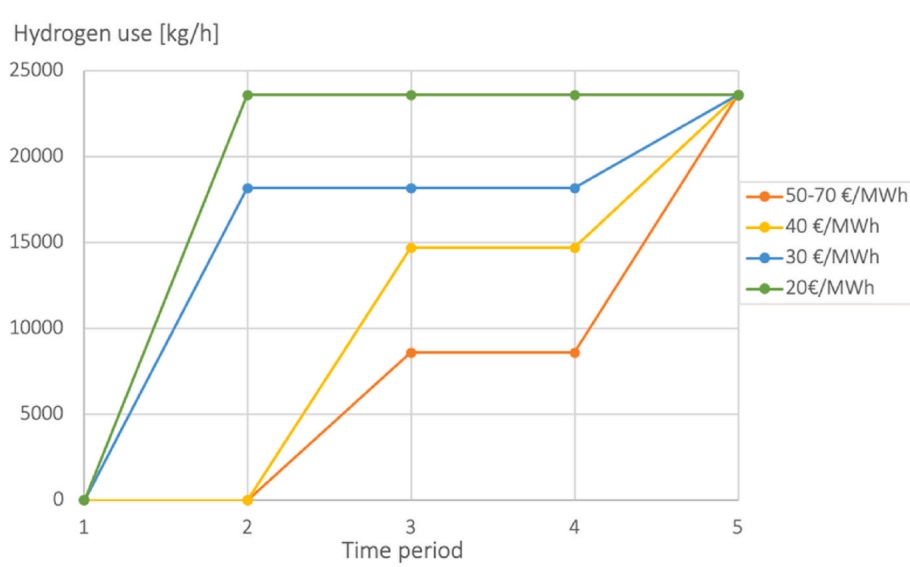

Fig. 11. Evolution of hydrogen demand when minimizing accumulated costs in Case 1.

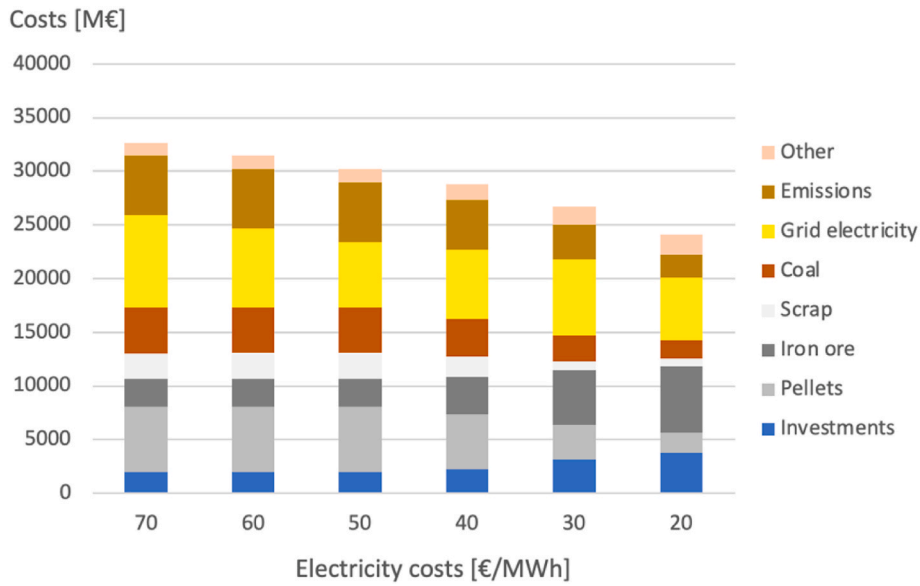

Fig. 12. Breakdown of total accumulated costs in Case 1.

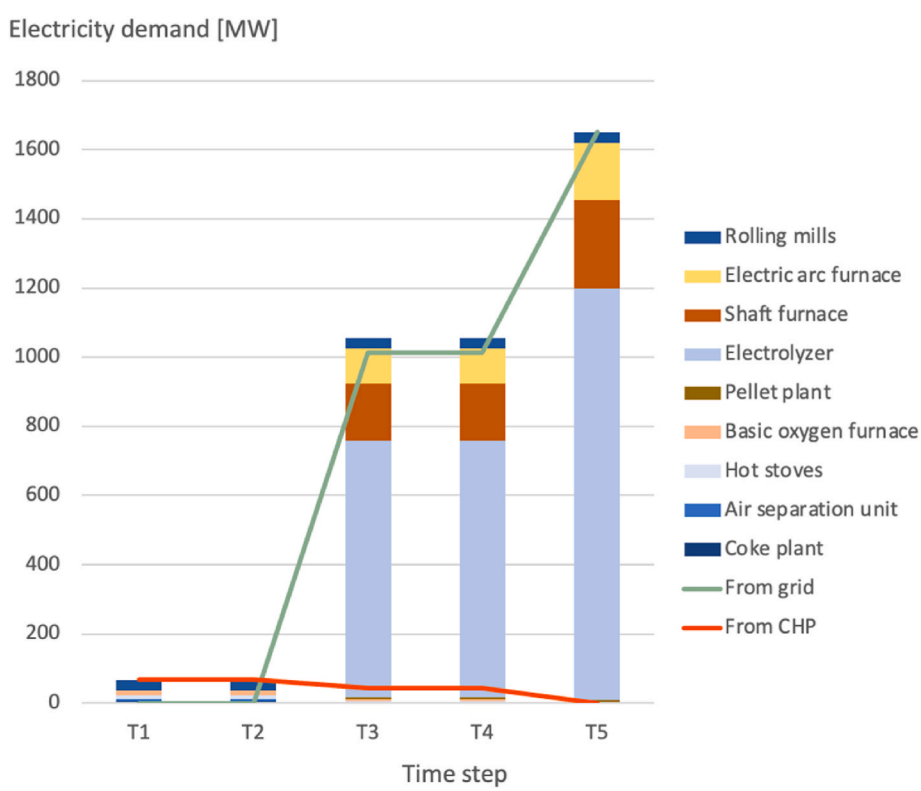

Fig. 13. Electricity sources and sinks in the Case 1 solution with 40 €/MWh electricity cost.

in the third period. With electricity costs of 30 €/MWh, one blast furnace is replaced with a shaft furnace and an EAF already in the second time period. With electricity costs of 20 €/MWh, both blast furnaces are replaced in the second time period, with two shaft furnaces and two EAFs. The solutions can be compared with a reference case in which steel production continues solely with the BF-BOF route. With electricity costs of 70 €/MWh, the solution of Case 1 features about 16 % higher accumulated costs and 20 % lower emissions than the reference case. With electricity costs of 20 €/MWh, the solution features about 15 % lower accumulated costs and 47 % lower emissions than the reference case. Feasibility regarding the transition time frame can partly be evaluated through the expected hydrogen demand (Fig. 11). Transitioning to the H2-DR route will in these cases eventually increase hydrogen demand from zero to nearly 24 000 kg/h, i.e., almost 210 000 t/a. In parallel, electricity demand increases from roughly 68 MW–1650 MW, and it is necessary to ask how quickly such an expansion could take place. As a crude estimate, if producing 260 t/h steel requires 1650 MW grid electricity, replacing all the steel production within the European Union (approximately 140 Mt in 2022 [37]) with this model solution would require roughly 100 GW additional grid electricity capacity.

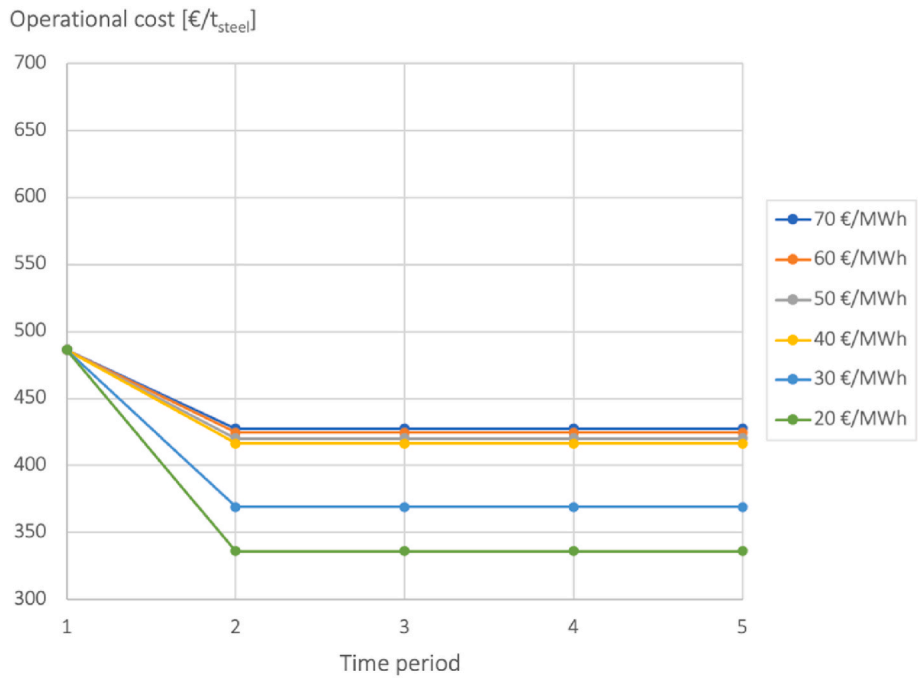

Fig. 14. Evolution of operational costs when minimizing accumulated costs in Case 2.

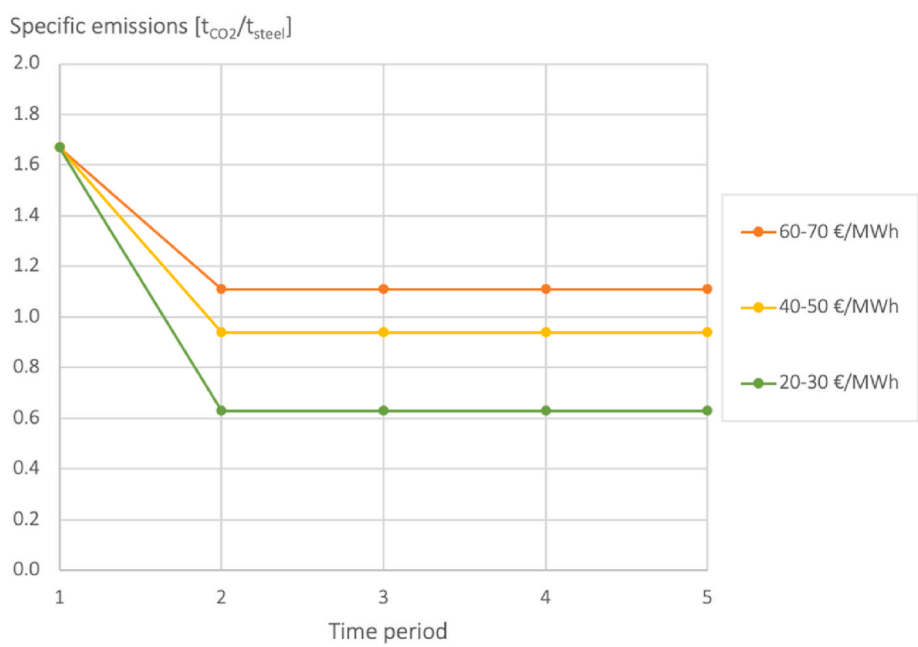

Fig. 15. Evolution of specific emissions when minimizing accumulated costs in Case 2.

3.3. Case 2 – alternative options

In a second test case, the model was given more freedom compared to Case 1, allowing blast furnace relining in periods 3 and 5 and scrap import up to 150 t/h for the EAF, as well as DRI imports. Resulting operational costs and specific emissions are shown in Figs. 14 and 15. Operational costs now decrease regardless of electricity costs as the option of charging an EAF with scrap reduces costs in all the solutions, despite relatively high prices assigned to scrap imports. Scrap imports constitute a major part of the total costs as seen in the total cost breakdown in Fig. 16. With electricity costs of 40–70 €/MWh, one blast furnace is replaced from the second time period onward with one EAF charged primarily with scrap, but also some imported DRI. In period 5, the remaining blast furnace is relined and continues operation. With electricity costs of 20–30 €/MWh, both blast furnaces are replaced in the second time period, with one shaft furnace and two EAFs charged with scrap and hydrogen-based DRI. This configuration reaches lower specific emissions than the solutions in Case 1, due to lower estimated emissions of recycling steel in an EAF compared with the H2-DR route with the assumed emissions from grid electricity.

If the objective function is changed to minimizing accumulated emissions, solutions favor building EAFs charged with scrap and externally bought DRI, leading to a system with operational costs 446 €/t_{steel} and emissions of 0.61 t_{CO2}/t_{steel} from the second time period onward

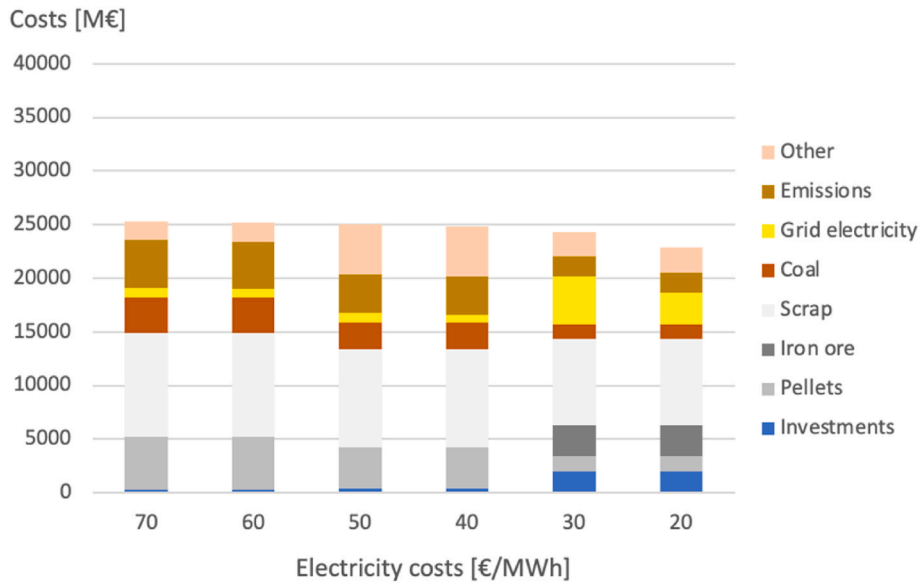

Fig. 16. Breakdown of total accumulated costs in Case 2.

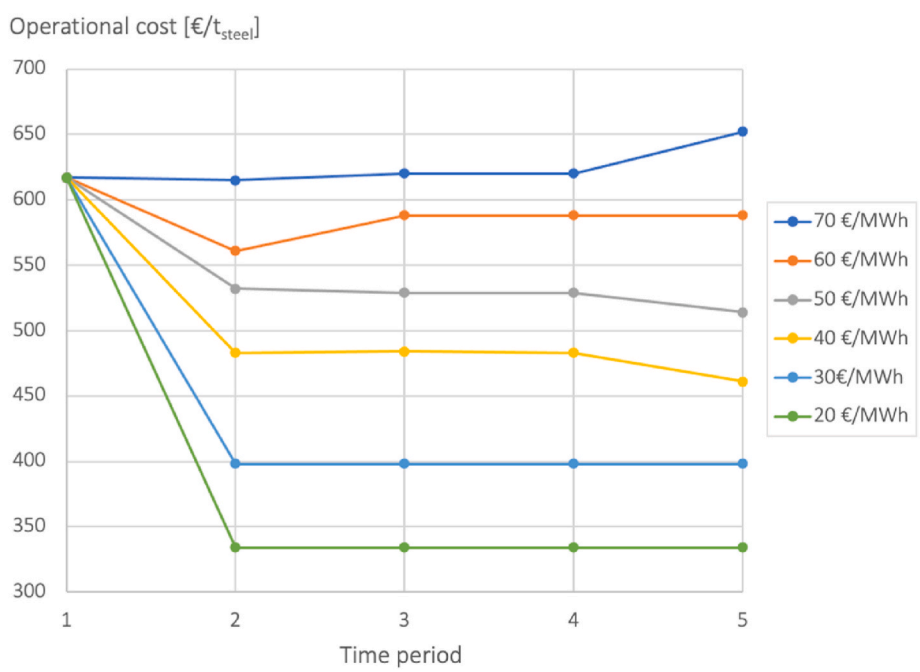

Fig. 17. Evolution of operational costs when minimizing accumulated costs in Case 3.

when electricity costs are 70 €/MWh. This solution depends on the emissions estimates for the external DRI and grid electricity, which were 0.4132 t_{CO2}/t_{DRI} and 0.089 t_{CO2}/MWh. If emissions from electricity are decreased to 0.075 t_{CO2}/MWh, solutions already favor construction of own shaft furnaces for DRI production, with operational costs 501 €/t_{steel} and emissions of 0.57 t_{CO2}/t_{steel} from the second time period onward.

3.4. Case 3 – forced transition with higher emissions costs

Case 3 has the same assumptions as Case 1, except with emissions costs increased to 150 €/t_{CO2}. Operational costs and emissions in the solutions are shown in Figs. 17 and 18, and a total cost breakdown in Fig. 19. Comparing with Case 1, costs are generally higher, but only marginally in the solutions with lower electricity costs, as they quickly transition to system configurations with lower emissions. Higher emissions costs also mean that transitioning to the H2-DR route lowers operational costs for electricity costs of 60 €/MWh or below compared with the BF-BOF route. Generally, costs after the transition are almost the same in Cases 1 and 3 in the final time step, as the system emissions are low at this point (see Fig. 20).

A notable situation in these solutions is with electricity costs 60 €/MWh, time steps 2–3. The configurations of this solution are shown in Table 8, along with electricity use in Fig. 21. Figs. 17 and 18 show how the system reaches lower costs and emissions in time step 2, with both blast furnaces in use, than in time step 3, when one blast furnace is decommisioned. The optimal solution opts for building a shaft furnace and EAF already in time step 2, and some shaft furnace DRI is fed to the blast furnaces, while the EAF is operated with part of its capacity. This creates a configuration with slighly lower emissions than that of time

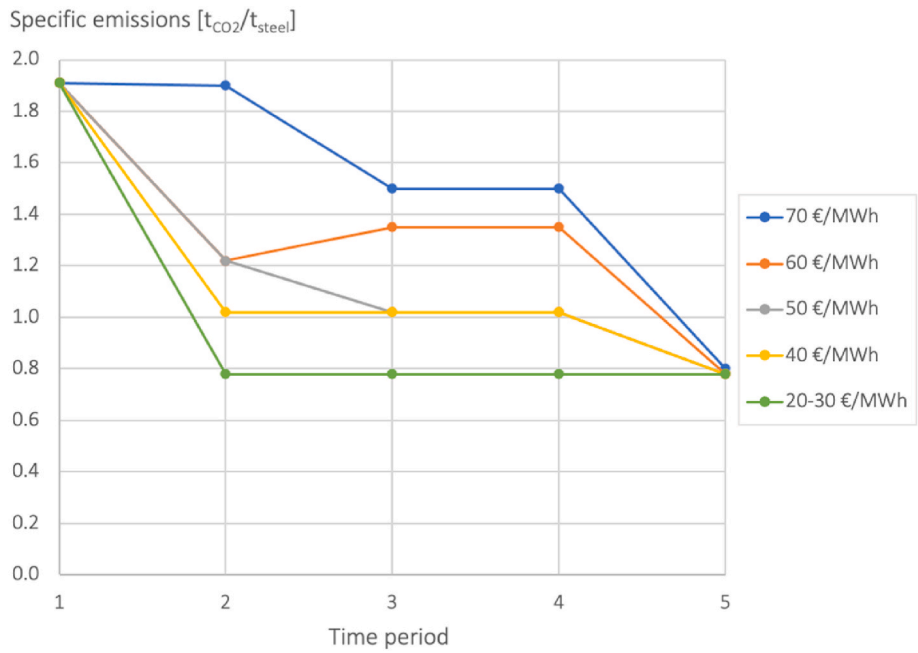

Fig. 18. Evolution of specific emissions when minimizing accumulated costs in Case 3.

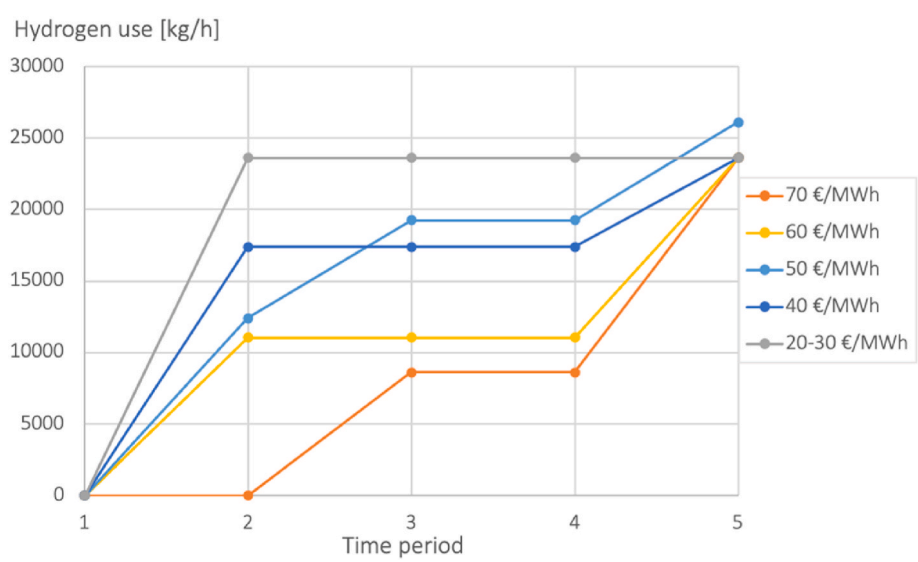

Fig. 19. Evolution of hydrogen demand when minimizing accumulated costs in Case 3.

step 3, when one of the blast furnaces no longer can operate.

4. Conclusions and future prospects

This paper has presented an optimization model for analyzing steel plant transition towards hydrogen-based steel production. The idea is to have a general and modifiable system model applicable in a wide variety of initial situations with different plant configurations for analysis of operation and investment decisions during upcoming decades. This feature is important since steel plants show differences with respect to raw materials and energy sources used, plant configuration and integration with the surrounding environment, raw material and energy costs, and emission penalties. The modelling principle is deemed feasible, as the quadratic form of the model is such that modern solvers can solve most problem instances very effectively to global optimality. Simplified surrogate models of more complex blast furnace and shaft furnace models were favorably incorporated in the system optimization model and this method can be extended to other system units as well if detailed models are available.

The example cases indicate that simple economic considerations favor use of EAFs and continued blast furnace use when electricity prices exceed 40 €/MWh, but the H2-SF route becomes competitive with lower electricity prices. Competitiveness of the H2-SF route is further supported if the emissions penalty is substantial. Regarding the extent of grid emission intensities affecting emissions from the H2-DR route, tests with the model suggest that grid emissions need to be less than around 0.3 tCO_2/MWh for the H2-DR route emissions to be lower than for corresponding production with the BF-BOF route. The modelling approach can flexibly be extended to evaluate a wide range of scenarios with different progressions of costs and other parameters over the selected time horizon. Varying parameter values, the modelling approach can be used to identify robust investment plans and system

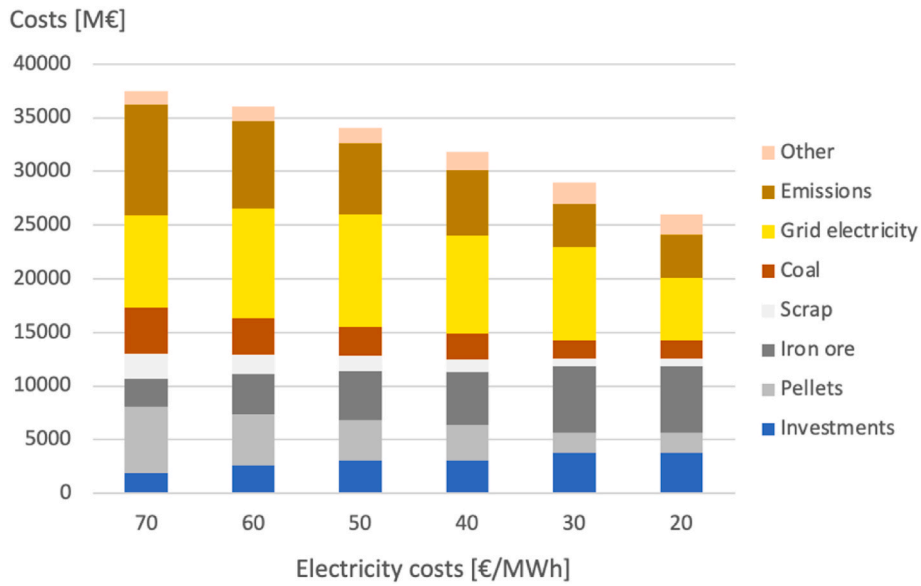

Fig. 20. Total accumulated cost breakdown in Case 3.

Table 8
System configuration in Case 3 solutions with 60 €/MWh electricity cost. The top half shows maximum capacities and hourly outputs, while the bottom half only shows outputs.

Unit	T1	T2	T3	T4	T5
	2 x 160 t/h 252 t/h	2 x 160 t/h 160 t/h	160 t/h 134 t/h	160 t/h 134 t/h	
		678 MW 136 kNm^3/h	678 MW 136 kNm^3/h	678 MW 136 kNm^3/h	1451 MW 290 kNm^3/h
		150 t/h 150 t/h	150 t/h 150 t/h	150 t/h 150 t/h	150 + 200 t/h 321 t/h
		150 t/h 101	150 t/h 129 t/h	150 t/h 129 t/h	150 + 150 t/h 277 t/h
		444 t/h 208 t/h	444 t/h 208 t/h	444 t/h 208 t/h	444 t/h 444 t/h
	277 t/h	176 t/h	147 t/h	147 t/h	
	105 t/h	51 t/h	57 t/h	57 t/h	
	84 MW_{el}	45 MW_{el}	45 MW_{el}	45 MW_{el}	
	14 kNm^3/h				
0	260 t/h	260 t/h	260 t/h	260 t/h	260 t/h

configurations that utilize old and new system units efficiently. Regression models in the example cases have been computed for given raw material compositions and limited plant capacities, so implementations of the modelling approach may require re-evaluation of relevant regression model variables and recalculation of model parameters according to specific needs in each case.

The general formulation of the system makes it possible to modify and add models of different units according to the modelled situation. Preferably, a more detailed EAF model could be implemented, possibly as another regression model that could consider varying flow rates of coal, lime and oxygen depending on EAF operation, and hot metal as an alternative feed. Larger hydrogen storage may be required at a steel plant with hydrogen production and should also be considered as an upcoming model addition. Shaft furnace models could be improved in several ways, e.g., with more detailed recycling modelling and alternatives for top gas utilization, options for different pellet qualities and for heating the input gas through combustion of gases from the process. Also, gas mixtures besides pure H_2 could be considered in the reduction gas. Availability of operational data from pilot facilities may in the future greatly enhance the reliability of the shaft furnace models. Additionally, excess heat from electrolysis could be utilized externally, e.g., in greenhouses, or by boosting it to a higher temperature using heat pumps.

Another relevant consideration is to include some dynamics regarding system operation during the time periods instead of assuming steady-state operation. This would increase the required computational efforts considerably, but they could still stay within reasonable limits as the model in its current form has short calculation times.

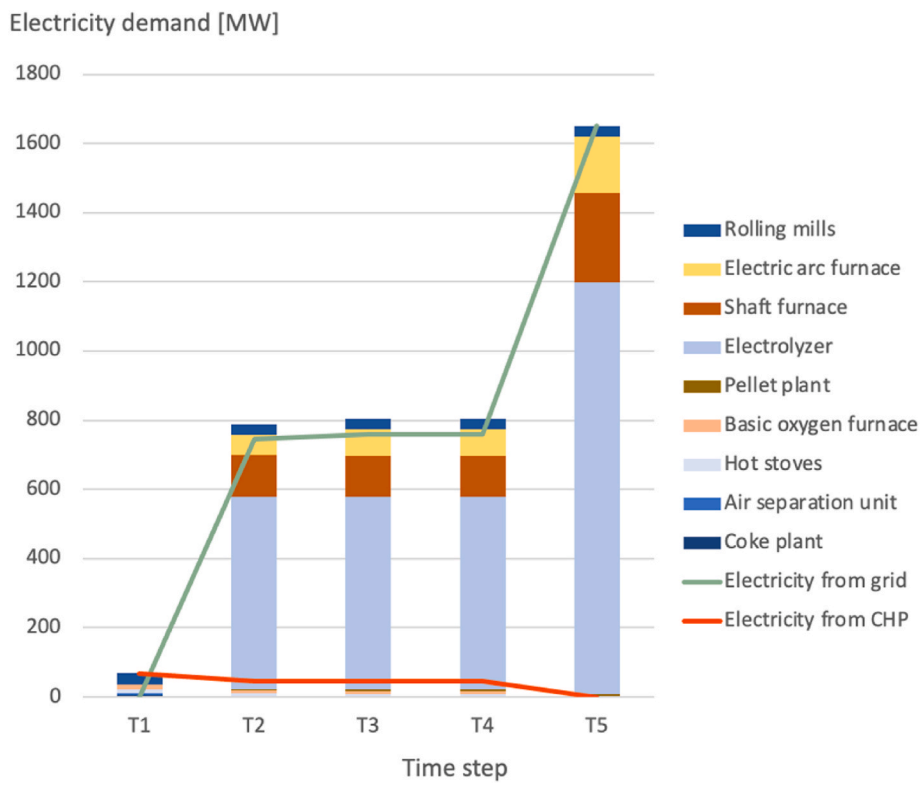

Fig. 21. Electricity sources and sinks in the Case 3 solution with 60 €/MWh electricity cost.

CRediT authorship contribution statement

Carl Haikarainen: Conceptualization, Formal analysis, Investigation, Methodology, Software, Visualization, Writing – original draft, Writing – review & editing, Data curation. **Lei Shao:** Methodology, Resources, Software. **Frank Pettersson:** Conceptualization, Methodology, Resources, Supervision, Validation, Writing – review & editing. **Henrik Saxén:** Conceptualization, Funding acquisition, Project administration, Resources, Supervision, Validation, Writing – review & editing.

Declaration of competing interest

The authors declare that they have no known competing financial interests or personal relationships that could have appeared to influence the work reported in this paper.

Data availability

The authors do not have permission to share data.

Acknowledgements

This research was funded by Business Finland and companies in the project Towards Fossil-free Steel (FFS) as well as by the Maximise H2 Enrichment in Direct Reduction Shaft Furnaces (MAXH2DR) project funded by Horizon Europe (Grant agreement 101058429). The authors wish to express their gratitude for the financial support.

References

[1] Wang P, Zhao S, Dai T, Peng K, Zhang Q, Li J, Chen W-Q. Regional disparities in steel production and restrictions to progress on global decarbonization: a cross-national analysis. Renew Sust Energ Review 2022;161:112367. https://doi.org/10.1016/j.rser.2022.112367.

[2] Wang RR, Zhao YQ, Babich A, Senk D, Fan XY. Hydrogen direct reduction (H-DR) in steel industry – an overview of challenges and opportunities. J Clean Prod 2021;329:129797. https://doi.org/10.1016/j.jclepro.2021.129797.

[3] Hybrit. 2022. www.hybritdevelopment.se/se/. [Accessed 19 August 2022].

[4] Primetals Technologies. 2021. www.primetals.com/press-media/news/hyfor-pilot-plant-under-operation-the-next-step-for-carbon-free-hydrogen-based-direct-reduction-is-done. [Accessed 19 August 2022].

[5] Thyssenkrupp. https://www.thyssenkrupp.com/en/newsroom/press-releases/pressdetailpage/climate-neutral-future-of-steel-production–real-world-laboratory-of-the-energy-transition-h2stahl-project-to-start-at-duisburg-site-of-thyssenkrupp-steel-129078. [Accessed 22 August 2022].

[6] Spreitzer D, Schenk J. Reduction of iron Oxides with hydrogen – a review. Steel Res Int 2019;90:1900108. https://doi.org/10.1002/srin.201900108.

[7] Patisson F, Mirgaux O. Hydrogen Ironmaking: how it works. Metals 2020;10:922. https://doi.org/10.3390/met10070922.

[8] Shao L, Zhang X, Zhao C, Qu Y, Saxén H, Zou Z. Computational analysis of hydrogen reduction of iron oxide pellets in a shaft furnace process. Renew Energ 2021;179:1537–47. https://doi.org/10.1016/j.renene.2021.07.108.

[9] Vogl V, Åhman M, Nilsson LJ. Assessment of hydrogen direct reduction for fossil-free steelmaking. J Clean Prod 2018;203:736–45. https://doi.org/10.1016/j.jclepro.2018.08.279.

[10] Bhaskar A, Abhishek R, Assadi M, Somehesaraei HN. Decarbonizing primary steel production: techno-economic assessment of a hydrogen based green steel production plant in Norway. J Clean Prod 2022;350:131339. https://doi.org/10.1016/j.jclepro.2022.131339.

[11] Pimm AJ, Cockerill TT, Gale WF. Energy system requirements of fossil-free steelmaking using hydrogen direct reduction. J Clean Prod 2021;312:127665. https://doi.org/10.1016/j.jclepro.2021.127665.

[12] Zaccara A, Petrucciani A, Matino I, Branca TA, Dettori S, Iannino V, Colla V, Bampaou M, Panopoulus K. Renewable hydrogen production processes for the off-gas valorization in integrated steelworks through hydrogen Intensified methane and methanol syntheses. Metals 2020;10:1535. https://doi.org/10.3390/met10111535.

[13] Angeli SD, Gossler S, Lichtenberg S, Kass G, Agrawal AK, Valerius M, Kinzel KP, Deutschmann O. Reduction of CO_2 emission from off-gases of steel industry by dry Reforming of methane. Angew Chem Int Ed 2021;60:11852–7. https://doi.org/10.1002/anie.202100577.

[14] Ghanbari H, Pettersson F, Saxén H. Optimal operation strategy and gas utilization in a future integrated steel plant. Chem Eng Res Design 2015;102:322–36. https://doi.org/10.1016/j.cherd.2015.06.038.

[15] Prina MG, Lionetti M, Manzolini G, Sparber W, Moser D. Transition pathways optimization methodology through EnergyPLAN software for long-term energy planning. App Energ 2019;235:356–68. https://doi.org/10.1016/j.apenergy.2018.10.099.

[16] Haikarainen C, Pettersson F, Saxén H. Optimized phasing of the development of a regional energy system. Energy 2020:118129. https://doi.org/10.1016/j.energy.2020.118129.
[17] Pettersson F, Saxén H. Model for economic optimization of iron production in the blast furnace. ISIJ Int 2006;46:1297–305. https://doi.org/10.2355/isijinternational.46.1297.
[18] Helle H. Towards sustainable iron- and steelmaking with economic optimization. Turku, Finland: Åbo Akademi University; 2014. Doctoral Thesis.
[19] Helle H, Helle M, Saxén H. Nonlinear optimization of steel production using traditional and novel blast furnace operation strategies. Chem Eng Sci 2011;66:6470–81. https://doi.org/10.1016/j.ces.2011.09.006.
[20] Huitu K, Helle M, Helle H, Kekkonen M, Saxén H. Optimization of Midrex direct reduced iron Use in ore-based steelmaking. Steel Res Int 2015;86. https://doi.org/10.1002/srin.20140091.
[21] Pikkuaho O. The potential Use of LNG in SSAB Raahe steelworks. Turku, Finland: Åbo Akademi University; 2020. Master's Thesis, https://urn.fi/URN:NBN:fi-fe20201221101795.
[22] Di Cecca C, Barella S, Mapelli C, Gruttadauria A, Ciuffini AF, Mombelli D, Bondi E. Thermal and chemical analysis of massive use of hot briquetted iron inside basic oxygen furnace. J Iron Steel Res Int 2017;24:901–7.
[23] David M, Ocampo-Martínez C, Sánchez-Peña R. Advances in alkaline water electrolyzers: a review. J Energ Storage 2019;23:392–403. https://doi.org/10.1016/j.est.2019.03.001.
[24] Sánchez M, Amores E, Abad D, Rodríguez L, Clemente-Jul C. Aspen Plus model of an alkaline electrolysis system for hydrogen production. Int J Hydr Energ 2020;45:3916–29. https://doi.org/10.1016/j.ijhydene.2019.12.027.
[25] Li F, Chu M, Tang J, Liu Z, Guo J, Yan R, Liu P. Thermodynamic performance analysis and environmental impact assessment of an integrated system for hydrogen generation and steelmaking. Energy 2022:122922. https://doi.org/10.1016/j.energy.2021.122922.
[26] Kirschen M, Badr K, Pfeifer H. Influence of direct reduced iron on the energy balance of the electric arc furnace in steel industry. Energy 2011;36:6146–55. https://doi.org/10.1016/j.energy.2011.07.050.
[27] Hay T, Visuri V-V, Aula M, Echterhof T. A review of mathematical process models for the Electric Arc furnace process. Steel Res Int 2021;92:2000395. https://doi.org/10.1002/srin.202000395.
[28] Pyomo. 2022. www.pyomo.org. [Accessed 21 December 2022].
[29] Gurobi. 2022. www.gurobi.com. [Accessed 21 December 2022].
[30] OECD. Steel market developments – Q2 2022. 2022. https://www.oecd.org/industry/ind/steel-market-developments-Q2-2022.pdf. [Accessed 2 September 2022].
[31] IRENA. In: Green hydrogen cost reduction: scaling up Electrolysers to Meet the 1.5°C Climate goal; 2020. https://www.irena.org/publications/2020/Dec/Green-hydrogen-cost-reduction. [Accessed 25 March 2024].
[32] Vartiainen E, Breyer C, Moser D, Medina ER, Busto C, Masson G, Bosch E, Jäger-Waldau A. True cost of solar hydrogen. Sol RRL 2021;6:2100487. https://doi.org/10.1002/solr.202100487.
[33] Motiva. In: CO_2-päästökertoimet (CO2 emissions coefficients, in Finnish); 2022. https://www.motiva.fi/ratkaisut/energiankaytto_suomessa/co2-paastokertoimet. [Accessed 14 October 2022].
[34] Van der Voet E, van Oers L, Verboon M, Kuipers K. Environmental implications of future demand scenarios for metals: methodology and application to the case of seven major metals, Supplementary materials. J Ind Ecol 2018;23:141–55. https://doi.org/10.1111/jiec.12722.
[35] Perpiñán J, Peña B, Bailera M, Eveloy V, Kannan P, Raj A, Lisbona P, Romeo LM. Integration of carbon capture technologies in blast furnace based steel making: a comprehensive and systematic review. Fuel 2023:127074. https://doi.org/10.1016/j.fuel.2022.127074.
[36] World Steel Association. In: Climate change and the production of iron and steel; 2021. https://worldsteel.org/wp-content/uploads/Climate-policy-paper-2021.pdf. [Accessed 27 January 2023].
[37] Statista. In: Annual production of crude steel in the European Union (EU-27) from 2009 to 2022; 2024. https://www.statista.com/statistics/550693/crude-steel-production-european-union/. [Accessed 9 April 2024].